Motor cooperation in bi-directional early endosome motility

Submitted by Martin Schuster

to the University of Exeter as a thesis for the degree of Doctor of Philosophy in Biological Sciences

February 2011

I certify that all material in this thesis which is not my own work has been identified and that no material has previously been submitted and approved for the award of a degree by this or any other University.

Martin Schuster

Abstract

In mammalian cells and fungi, early endosomes form a dynamic compartment that undergoes bi-directional motility along microtubules. Previous work has shown that in the model system *Ustilago maydis* early endosome motility involves the opposing motor proteins dynein and kinesin-3. Here I performed a detailed analysis of the role of the motors in early endosome motility, using quantitative live cell imaging of kinesin-3, dynein and the endosomal GTPase Rab5a. In the first part of my work, I analysed the role of dynein at MT plus-ends, where the motor forms a strong accumulation that was thought to be involved in capturing early endosomes. I could demonstrate that ~55 dynein motors build up the dynein accumulation. In collaboration with Ms. Congping Lin and Prof. Peter Ashwin (Institute for Mathematics, Exeter), I found theoretical evidence that ~25 dynein motors concentrate and leave the plus-ends stochastically. In addition, dynein motors are captured by an interaction of dynactin and the plus-end binding protein EB1. Together both mechanisms increase the number of motors, which ensures that EEs will be loaded onto dynein before they reach the end of their track. In a second project, I provide evidence that loading of dynein is not restricted to the plus-ends. Instead, dynein leaves the plus-ends and is able to bind to kinesin-3 delivered early endosomes, which changes their transport direction from anterograde to retrograde. Kinesin-3 remains bound to these retrograde EEs. When dynein leaves the organelle, it switches back to anterograde motility. Interestingly, a single dynein wins over three to five kinesin-3 motors. I discuss these findings in the light of current motor cooperation concepts. In a third part, I demonstrated that kinesin-3 has an unexpected role in long-range retrograde endosome motility. In contrast, dynein is only responsible for the distal 10-20 µm. This is possible because most of the hyphal cells contain a symmetric and bi-polar MT array. This MT organization is reminiscent of that in dendrites. Kinesin-3-based retrograde motility is required to mix the organelles and might support long-range communication between both cell poles.

Table of contents

List of Figures

List of Tables

Author's declaration

This work was undertaken with the help of co-workers.

Chapter 2:

Prof. Peter Ashwin and Congping Lin have done all mathematical modelling and the non-linear regression analysis.

Dr. Sreedhar Kilaru generated the following plasmids and strains: pNup214-2G, pNup214-3G, pNup2-G, pcrgDya1$^{32-62}$, pcrgDya1$^{32-62Q35E}$ and pcrgPeb1$^{211-268}$, FB2N214G$_3$, FB2N107G_N214G$_2$, FB2N107G_N214G$_3$, FB2N107G_N214G$_3$_N2G, AB33G$_3$Dyn2_rEB1$^{211-268}$, AB33 G$_3$Dyn2_rDya1$^{32-62}$ and AB33 G$_3$Dyn2_rDya1$^{32-62\ Q35E}$

Prof. Nicholas J Severs preformed the freeze-fracture transmission electron microscopy to visualise nuclear pores.

Prof. Gero Steinberg analysed data, provided overall project management and supervision and wrote the manuscript.

Chapter 3:

Prof. Reinhard Lipowsky intensively discussed the data and suggested new experiments.

Marcus-Alexander Assmann and Prof. Peter Lenz developed the mathematical model.

Prof. Gero Steinberg analysed data, provided overall project management and supervision and wrote the manuscript.

Chapter 4:

Dr.Sreedhar Kilaru generated of a temperature-sensitive *kinesin-3* mutant and the plasmids pKin3^{ts}, pKin3^{ts}G, potagRRab5a and pKin3G_H. He also generated the following strains: AB33Kin3G, AB33ΔKin3_Kin3^{ts}G, AB33ΔKin3_Kin3^{ts}G_tagRRab5a, AB33ΔKin3_Kin3^{ts}_G3Dyn2 and AB33ΔKin3_Kin3^{ts}_paGFP-Rab5a and AB33_ΔKin3_GRab5a.

Dr. Gero Fink has analyzed the degree of MT-bundling.

Dr. Jerome Collemare analyzed the co-localization of early endosomes and kinesin-3-GFP, aquired the movie showing long-range motility of early-endosomes and generated strain AB33ΔKin3_Kin3G_ChRab5a.

Yvonne Roger generated strain AB33ΔKin3_rDyn1_GRab5a and analyzed the co-localization of early endosomes and dynein (Figure 5A).

Prof. Gero Steinberg analysed data, provided overall project management and supervision and wrote the manuscript.

I would like to thank all co-author for there support and help.

Acknowledgements

First and foremost, I would like to thank Prof. Gero Steinberg for allowing me to study in his research group, and for being an excellent supervisor over the last years. I'm thankful for his enthusiasm, knowledge, help, trust and the way he pushed me to my limits.

Thanks to all colleagues I have worked with, in particular the co-Authors of the article, without them, this work would not be as good as it is now.

I would like to thank Sam, Yvonne, Steffi and Natalie for their friendship, help and the little scary jokes between the experiments.

I'm grateful to my parents and parents-in-law for there support to me and my family especially during the last year.

Finally, I offer my deepest thanks to my wife Mandy for being with me and for all the support and strength she gave me during the last hard years. I would also like to thank my two children Fynn and Annabel for being like they are and that they gave me the possibility to relax and unwind outside the lab.

Thank you all

Abbreviations

aa	amino acid
α anti-	*(antibodies)*
ATP	adenosinetriphosphate
a.u.	arbitrary unit
ble^R	phleomycin-resistance-cassette
bp	base pair(s)
cbx-locus	gene locus of the iron-sulphur subunit of the succinate-dehydrogenase from *Ustilago maydis*
cbx^R	carboxin-resistance-cassette
CCCP	carbonyl cyanide 3-chlorophenylhydrazone
CM	complete medium
crg - promoter	conditional arabinoseinduced promoter
C-terminal	carboxy-terminal
DIC	differential interference contrast
DNA	desoxyribonucleic acid
dNTP	desoxynucleotides
dya1	dynactin subunit $p150^{Glued}$
Dyn1	dynein 1 from *U. maydis*
Dyn2	dynein 2 from *U. maydis*
EE	early endosome
eGFP	enhanced green fluorescent protein
ER	endoplasmic reticulum
FRAP	fluorescent recovery after photo-bleaching
GFP	green fluorescent protein

h	hour
HDEL	endoplasmic reticulum retention signal
hyg^R	hygromycin-resistance-cassette
kb	kilo bases
kD	kilo Dalton
kin1	kinesin-1
kin3	kinesin-3
mCherry	monomeric Cherry fluorescent protein
min	minute
ml	millilitre
µl	microlitre
µm	micrometer
µM	micromolar
mRFP	monomeric red fluorescent protein
ms	millisecond
MT	microtubule
mW	milli Watt
n	sample size
nat^R	nourseothricin-resistance-cassette
nar - promoter	conditional nitrate reductase promoter
NLS	nuclear localization signal
nm	nanometre
N-terminal	amino-terminal
Nup	nucleoporin
ORF	open reading frame
otef-promoter	promoter of the translation elongation factor 1 of *U. maydis*

p	probability
pamgfp	photoactivatable monomeric green-fluorescent protein
PCR	polymerase chain reaction
P*crg*	promoter of the arabinase gene from *U. maydis*
peb1	EB1-like plus-end binding protein
rab5a	small endosomal Rab5-like GTPase
RFP	red fluorescent protein
rpm	rounds per minute
RT	room temperature
s	second
s.e.m	standard error of the mean
tagRFP	red fluorescent protein
Tub1	α-tubulin from *U. maydis*
^{TS}	temperature-sensitive allele
U	Unit
wt	wildtype
YFP	yellow fluorescent protein

Introduction

Bidirectional motility of organelles is a common phenomenon in many cell types (Wedlich-Söldner et al., 2000a; Miaczynska et al., 2004; Abenza et al., 2009). It is mainly mediated by the molecular motors kinesin-1, kinesin-3 and dynein (Wedlich-Söldner et al., 2002a; Vale, 2003; Hirokawa & Takemura, 2004). In fungi, motility of early endosomes seems to be essential for hyphal growth and it is mediated by dynein and kinesin-3 (Wedlich-Söldner et al., 2002a; Lenz et al., 2006). In this study, I used the basidiomycete fungus *Ustilago maydis* to extend our understanding of the molecular basis of bi-directional motility of early endosomes.

1.1 Bi-directional Transport

Diffusion is suitable to distribute small molecules over short distances up to 20 nm (Agutter & Wheatley 2000) but it is not an efficient way for transporting vesicles or organelles to overcome larger distances in eukaryotic cells (Howe, 2005). Organelle motility over larger distance involves energy-dependent directed transport (Paschal et al., 1987; Vale, 2003; Shimmen, 2007). Cells have developed several mechanisms for active large-scale transport of proteins, RNAs and organelles. Such mechanisms include cytoplasmic streaming (Vits, 1991; Shimmen, 2007) and motor-based transport along the fibres of the cytoskeleton (Vale, 2003; Hirokawa & Takemura, 2004; Mische et al., 2007; Hartman et al 2009). With regard to intracellular transport, bi-directional motility of organelles along microtubules is best understood (Vale, 2003; Hirokawa & Takemura, 2004; Welte, 2004).

1.2 Molecular Basis of Organelle Transport along microtubules

1.2.1 The Microtubules

Microtubules are polymers of α- and β-tubulin dimers with a diameter of 25 nm. Microtubules are polar structures and there plus ends, expose β-tubulin subunits (Nogales et al., 1999). The less dynamic minus ends are normally anchored at a microtubule organizing centre, where another iso-form of tubulin, γ-tubulin, supports polymerization (Job et al., 2003; Oakley 2004). The γ-tubulin complexes with associated proteins forms a circular structure, known as the γ-tubulin ring complex, which acts as a template to start polymerization (Job et al., 2003). From the microtubule organizing centres the microtubules polymerise by adding α/β-tubulin dimers to the growing protofilaments. The plus ends of microtubules are highly dynamic and can switch between growing and shrinking (Mitchison and Kirschner 1984; Desai & Mitchison, 1997; Nogales et al., 1999; Dixit & Ross, 2010).

Microtubules have essential functions in intracellular transport. They build the tracks along which molecular motors move there cargo through the cell (Vale, 2003; Hirokawa & Takemura, 2004). They also build the mitotic and meiotic spindle apparatus and therefore have crucial roles in chromosome segregation during mitosis and meiosis (Gadde and Heald, 2004; Fink et al., 2006). The orientation of microtubules is of importance for the organization of eukaryotic cells. In neurons, the axons contain a uniform microtubule array that extends its plus ends towards the growth cone (Burton & Paige, 1981; Heidemann et al., 1981). In neuronal dendrites, the microtubule array is non-uniform with a uni-polar array near the dendric cone and bi-polar oriented microtubules in the rear part of the dendrite (Baas et al., 1988; Baas et al., 1991). The difference in

microtubule organization allows the minus end-directed molecular motor dynein to sort Golgi membranes into the dendrites but prevents transport of this compartment into the axons (Zheng et al., 2008). Thus, the orientation of microtubules underlies the use of molecular motors in organelle transport. In hyphae of filamentous fungi the plus ends of microtubules are orientated to the growth region (Schuchardt et al., 2005; Xiang et al., 2000). This is thought to allow kinesin motors to support polarized hyphal growth (Konzack et al., 2004; Schuchardt et al., 2005).

1.2.2 The molecular motors in long distance organelle transport

Molecular motors are enzymes, which hydrolyse ATP to move their cargo along the fibres of the cytoskeleton. There are two microtubule-based motor families known, the kinesins and dynein motors, which differ in their composition and in their transport direction along the microtubule. Dynein moves its cargo towards the minus-ends, whereas most kinesins travel towards the plus ends (Vale, 2003) It was shown that both plus end and minus end directed molecular motors are involved in transport of numerous cargo, including secretory vesicles (Wacker et al., 1997; Manneville et al., 2003), mitochondria (Hollenbeck et al., 1996, Chada et al., 2003), endosomes (Hollenbeck et al., 1993; Valetti et al., 1999; Murray et al., 2000) and virus particles (Smith et al., 2001; McDonald et al., 2002). By moving the cargo bidirectionally, the cell is able to equally distribute organelles (Maly 2002) or position organelles (Feiguin et al., 1994; Hirokawa et al., 1998; Januschke et al., 2002), but might also correct transport mistakes (Ally et al., 2009). In eukaryotes dynein, kinesin-3 and kinesin-1 are the most common motors for intracellular transport processes (Vale, 2003).

1.2.2.1 Kinesin-1

Kinesin-1 is the founding member of the kinesin motors and therefore was initially named "conventional kinesin". It was identified in the mid 1980s in various organisms and cell types including squid and nervous tissue and sea urchin eggs (Brady, 1985; Scholey et al., 1985; Vale et al., 1985). Kinesin-1 was also the first membrane transporter isolated and characterised in ascomycete, basidiomycete and zygomycete fungi (Steinberg and Schliwa, 1995, Steinberg and Schliwa, 1996; Steinberg, 1997; Steinberg et al., 1998). Kinesin-1 consists of a dimer of heavy chains that form a N-terminal motor domain and a globular tail domain, which are linked by a stalk consisting of two coiled-coil regions. In animals, the kinesin-1 tail binds light chains (Kuznetsov et al., 1989), which are not found in fungal kinesin-1 (Steinberg and Schliwa, 1996; Steinberg, 1997; Steinberg et al. 1998). The light chains support binding to the cargo and might be partly involved in cargo selectivity (Hirokawa, 1998). In general, kinesin-1 is thought to transport organelles and transport vesicles (Hirokawa, 1998), but it is also involved in transport of mRNAs (Brendza et al., 2000) and intermediate filaments (Prahlad et al., 1998). The tail is thought to support cargo interaction (Seiler et al., 2000), but also folds back to the motor head thereby inactivating the motor (Cai et al., 2007; Hackney & Stock 2008). Conventional kinesin has been extensively studied in *U. maydis* (Lehmler et al., 1997; Steinberg et al,. 1998; Schuchardt et al., 2005), *Neurospora crassa* (Steinberg et al,. 1995; Steinberg et al,. 1996; Seiler et al,. 1997; Seiler et al., 2000) and *Nectria haematococca* (Wu et al., 1998). In these organisms, kinesin-1 is essential for polarized secretion and hyphal growth (Seiler et al,. 1997). It has also functions in vacuole formation (Steinberg et al,. 1998) and the localisation of organelles (Wu et al., 1998). More recently it was found that kinesin-1 is involved in

targeting dynein to the microtubule plus ends (Zhang et al., 2003; Lenz et al., 2006).

1.2.2.2 Kinesin-3

Kinesin-3 motors were first found in a mutant screen of *C. elegans* (Hall and Hedgecock, 1991), where a mutation in Unc104 inhibited the transport of synaptic vesicles in motor neurons. First reports of this kinesin family suggest that they are mainly monomeric (Nangaku et al., 1994; Okada et al., 1995). However, subsequent studies demonstrated that kinesin-3 can dimerize (Tomishige et al., 2002; Hammond et al., 2009). Similar to kinesin-1, the members of this familiy of motors contain a N-terminal motor domain and an extended tail that is thought to bind to membranes (Klopfenstein et al., 2002). The tail consists of two highly conserved domains. First, a fork head homology (FHA) domain with unknown function. It was suggested that the FHA domain is involved in dimerization and thereby could have a regulatory function (Lee et al., 2004). Second, it contains a pleckstrin homology (PH) domain. This domain is found in a wide range of proteins (Hemmings et al., 1993; Gibson et al., 1993; Wang et al., 1995). The PH domain is reported to interact with membranes by phosphoinositol lipid binding (Klopfenstein et al., 2002). The *Drosophila* kinesin-73, *C. elegans* CeKLP-4, mouse KIF13B, and human GAKIN belong also to the KIF1A family and contain a third domain, a Cap-Gly domain (Vallee, 2003), which is known to bind microtubules (Weisbrich et al., 2007; Sun et al., 2009). Kinesin-3 is an important membrane transporter in neurons (Yonekawa et al., 1998; DeGiorgis et al., 2008) and is important for the regulation of neuronal cell polarity (Horiguchi et al., 2006). In lower eukaryotes, such as *Dictyostelium*

discoideum (Pollock et al., 1999) and *U. maydis* (Wedlich-Söldner et al., 2002a), the kinesin-3-like kinesins are involved in early endosomes motility.

1.2.2.3 Dynein

Dynein is a large motor complex consisting of a dynein heavy chain, two light intermediate chains, two intermediate chains and the light chains Tctex1/rp3, road block and LC8. It was first discovered as the force generating compound of the axonemal cylinder in cilia of *Tetrahymena cilia* (Gibbons and Rowe, 1965), but subsequently found in numerous organisms including humans, animals and fungi (Paschal and Vallee, 1987; Hirokawa, 1998; Straube et al., 2001). Paschal and colleague identified cytoplasmic dynein as a protein that generates minus end directed motility in non-ciliated cells (Paschal et al., 1987). The dynein heavy chain forms the core of the complex. It contains a large C-terminal motor domain with six AAA domains that, together with an additional domain, form a ring like structure (Samso et al., 1998). Only the first four domains take part in binding and hydrolysing ATP, while the other may have structural functions (King 2000). The N-terminal part of the dynein heavy chain contains the dimerization domain as well as the interaction sites of the associated proteins, which include two light intermediate chains, two intermediate chains and the light chains Tctex, roadblock and LC8 (Habura et al., 1999; Tynan et al., 2000). Dynein serves many important functions in the cell. It is involved in minus end directed organelle transport in animal cells (Hirokawa, 1998; Hirokawa & Takemura, 2005) as well as in filamentous fungi (Wedlich-Söldner et al., 2002a; Lenz et al., 2006 Abenza et al., 2009; Zhang et al., 2010,). Dynein is also involved in the positioning of the Golgi (Corthesy-Theulaz et al., 1992; Harada et al., 1998), the endoplasmic reticulum (Allan, 1995; Wedlich-Söldner

et al., 2002b) or the nuclei (Bloom, 2001; Straube et al., 2001; Tsujikawa et al., 2007; Finley et al., 2008; Roca et al., 2010). It also has functions in mitosis to position the spindle and pulling on astral microtubules (Yeh et al., 1995; Carminati et al., 1997; Heil-Chapdelaine et al., 2000; Lee et al., 2003; Lee et al., 2005; Sheeman et al., 2003; Fink and Steinberg 2006). Dynein is often associating with the dynactin complex, which binds to the dynein heavy chain via the light intermediate chains. The dynactin complex was initially found as a regulator of organelle transport (Schroer et al., 1991). Dynactin is considered to be a processivity factor that increases the run length of dynein on microtubules (King and Schroer, 2000; Culver-Hanlon et al., 2006; Kardon et al., 2009). The dynactin complex can also foster binding to cargos, which is illustrated by the interaction of the dynactin compound dynamitin that binds to bicaudal on Golgi membranes in mammalian cells (Hoogenraad et al., 2001). An important subunit of the dynactin complex is the $p150^{glued}$ subunit. In epithelial cells and fibroblasts, it was shown that this subunit interacts with the plus end binding protein EB1 (Ligon et al., 2003; Honnappa et al., 2006; Akhmanova and Steinmetz, 2008) and anchors the dynactin complex at MT plus ends. After release, dynactin recruits dynein (Vaughan et al., 2002), thereby assembling the retrograde transport machinery, which moves early endosomes (Valetti et al., 1999), Golgi membranes (Vaughan et al., 2002; Vaughan, 2005) or melanophores (Lomakin et al., 2009). However, the assembly of the dynactin-dynein complex might already happen at the microtubule plus ends, as it was shown that cytoplasmic dynein itself concentrates at MT plus ends in mammalian cells (Kobayashi and Murayama, 2009) and fungi (Lee et al., 2003; Sheeman et al., 2003; Xiang, 2003; Zhang et al., 2003; Lee et al., 2005; Lenz et

al., 2006; Abenza et al., 2009; Zhang et al., 2010). Why dynein concentrates at the microtubule plus ends is not known.

1.3 Motor cooperation in bidirectional organelle transport

1.3.1 Model systems for bi-directional motility

The understanding of the way by which motors mediate bi-directional motility is mainly based on studies in a few model systems. An important cell system are melanophores, in which melanosomes move to change the colour of these pigment cells. The movement of melanosomes and the mechanism and regulation of this process is well described (reviewed in Nascimento et al., 2003). Cytoplasmic dynein moves them in minus end direction which leads to aggregations (Nilsson et al., 1997). Kinesin-2 (Tuma et al., 1998) and the actin motor myosin-V (Rogers et al., 1998) share forces to take melanosomes outward thereby allowing an even dispersion of the pigments. All motors are constantly bound to the organelle, allowing motor cooperation in a tug-of-war (Gross et al., 2002a). Another system is intraflagellar transport in the cilia of *Caenorhabditis elegans.* In this system dynein and kinesin-2 cooperate to move particles along the flagellum in a bidirectional fashion (Scholey 2003; Pedersen et al., 2006). Again, these motors are permanently bound to the cargo. Another well studied system are neuronal cells. In the Drosophila motor axons dynein and kinesin-1 moves mitochondria bidirectional (Pilling et al., 2006). UNC-104/Kif1 a kinesin-3 related kinesin was found to move vesicles (Barkus et al., 2008), whereas dynein is the main motor for retrograde early endosome motility in axons (Vale, 2003; Hirokawa & Takemura, 2004; Ha et al., 2008). Furthermore, the studies on *Drosophila* lipid droplet motility (Welte et al., 1998, Gross et al., 2002b) and the lower eukaryote *Dictyostelium discoideum*

(Soppina et al., 2009, Klopfenstein et al., 2003) have provided important insight in how motors cooperate in bi-directional motility.

1.3.2 Concepts of motor cooperation in bidirectional organelle transport

Initially, three different models were discussed of how motors work together to mediate bidirectional motility of cellular cargo (Gross, 2004; Welte, 2004). In the exclusionary presence model, only one kind of motor is present on the organelle at a given time. A switch in direction requires an exchange of the motors on the cargo. While this is an attractive concept, evidence for such a scenario is missing. The coordination model suggests that both sets of motors are present on the cargo but only one is active, whereas the opposite motor is inactivated and not attached to the track. This scenario requires a regulatory complex that controls the activation of both opposing motors. In a third scenario, the tug-of-war model, both minus and plus directed motors are present on the cargo and both are active at the same time. In this scenario the motors compete with each other, and the stronger motor takes over for directed motility. The opposing motor, however, can take over, thereby supporting bidirectional motility. Intensive work on motor cooperation in numerous model systems (see above) has demonstrated that regulatory proteins like kinases (Deacon et al., 2005; Guillaud et al., 2008), dynactin (Deacon et al., 2003) and other factors (Welte et al., 1998; Welte et al., 2005; Larsen et al., 2008) play a role in the control of bidirectional organelle traffic. However, increasing evidence accumulates for tug-of-war based mechanisms (Soppina et al., 2009; Hendricks et al., 2010). These experimental studies have gained support by theoretical evidence showing that stochastic tug-of-war can mediate bidirectional organelle motility (Müller, et al., 2008; Welte & Gross, 2008; Zhang, 2009). Thus, a combination

of the coordination and the tug-of-war scenario seems to be most likely. In both scenarios, the motors that counteract are simultaneously bound to the organelle.

1.4 Early endosomes

One of the best studied examples of bidirectional organelle transport is motility of early endosomes. These organelles were shown to move along microtubules *in vitro* (Murray et al., 2000), in neurons (Ha et al., 2008; Hirokawa & Takemura, 2004), in *D. discoideum* (Soppina et al., 2009) and in hyphae of filamentous fungi (Wedlich-Söldner et al., 2000; Higuchi et al., 2006; Penalva, 2010). Early endosomes are characterised by the small Rab-GTPases Rab4 and Rab5 (Gorvel et al., 1991; Bucci et al., 1992) and by the specific lipid PIP3 (Christoforidis et al., 1999; Behnia and Munro 2005). Rab-GTPases can serve as adapters for molecular motors (Nielsen et al., 1999; Seabra & Coudrier 2004). The primary function of early endosomes is to sort the internalized molecules to different cellular destinations. Early endosomes are therefore a focal point of the endocytic pathway. The majority of internalized molecules are recycled from early endosomes back to the plasma membrane (Koval and Pagano 1989). In an alternative pathway early endosomes maturate to late endosomes and thereby sort material to the vacuoles/lysosomes for degradation. (Berón et al., 1995; Alvarez-Dominguez & Stahl 1999). Early endosomes move within the cell (Nielsen et al., 1999; Clarke et al., 2002). This transport occurs along microtubules and involves kinesins and dynein (Aniento et al., 1993; Wedlich-Söldner et al., 2002a; Loubéry et al., 2008). Recently, the model fungus *Ustilago maydis* became a valuable system to study long-range motility of EEs (Wedlich- Söldner et al., 2000; Wedlich-Söldner et al., 2002a; Lenz et al., 2006).

1.5 The model fungus *Ustilago maydis*

The basidiomycete fungus *Ustilago maydis* has a long history as a model organism in cell biology. The molecular mechanism of DNA recombination was initially described in this fungus (Holliday 1964; Holliday 2004). *U. maydis* is a dimorphic fungus and an important pathogen on maize that induces the formation of tumours at the stem, the leaves and in the corncob of the plants. (Banuett & Herskowitz, 1996). In soil and under laboratory conditions, *U. maydis* grows as haploid yeast-like sporidia. On the plant surface, two compatible cells can recognise each other and can switch to hyphal growth (Bölker et al., 1992). The resulting hyphae can reach a length of more then 100µm and fuse to form an infectious dikaryotic filament (Snetselaar et al., 1996). The dikaryotic hyphae can enter the plant tissue and infect the plant. The fungus grows and proliferates within the plant. This leads to the induction of plant tumours, within diploid teliospores are made. These spores are released and subsequently form haploid sporida (Banuett & Herskowitz, 1996).

The genome of *U. maydis* has been sequenced (Kämper et al., 2006) and numerous molecular tools are established for it (Steinberg and Perez-Martin, 2008). A genetic screen for morphological mutants identified the gene Yup1, which, when defective, causes defects in polarized growth (Wedlich-Söldner et al., 2000). Yup1 was found to be a putative t-SNARE on early endosomes that controls the fusion with endocytic transport vesicles. Interestingly, the early endosomes moved rapidly along microtubules (Wedlich-Söldner et al., 2000). Motility was blocked when microtubules were disrupted (Wedlich-Söldner et al., 2000), suggesting that kinesins and dynein mediate bidirectional motions of early endosomes. In *U. maydis* hyphae, the microtubules form long tracks that

often form bundles (Steinberg et al., 2001). Using Peb1, an EB1 homologue in *U. maydis,* it was shown that only microtubule plus ends reach into the hyphal apex (Schuchardt et al., 2005). Consequently, a kinesin was expected to support early endosome motility towards the hyphal tip. The genome of *U.maydis* encodes for 10 kinesins (Schuchardt et al., 2005) and one dynein (Straube et al., 2001). It was reported that only kinesin-1 (Kin1) and kinesin-3 (Kin3) are required for filamentous growth and both motors are up-regulated in hyphal cells. Indeed, kinesin-1, kinesin-3 and dynein are involved in bidirectional motility of early endosomes in *U. maydis*.

1.6 The role of kinesin-1, kinesin-3 and dynein in early endosome motility in *U. maydis*

Kinesin-1 is a major transporter of organelles in all eukaryotic cells (see above). It was therefore tempting to speculate that kinesin-1 supports early endosome motility. However, deletion of kinesin-1 resulted in an accumulation of the organelles at the hyphal tip, where the plus ends of microtubules are located (Lenz et al., 2006). This suggested that plus end-directed transport of early endosomes was even stronger in the absence of the plus end motor kinesin-1. The solution to this contradiction was the finding that kinesin-1 transports dynein to microtubule plus ends (Lenz et al., 2006), a result first described in the fungus *Aspergillus nidulans* (Zhang et al., 2003; Zhang et al., 2010). The motor for the early endosomes was found to be kinesin-3 (Wedlich-Söldner et al., 2002a) which transports the organelles towards the plus ends at the hyphal tip. Here, kinesin-1-dependent delivery of dynein helped to build a dynein accumulation that is thought to be involved in loading of the organelles to the retrograde machinery. Why the dynein concentrates at microtubule plus ends

was not known, but it was speculated that dynein remains there inactive until the arriving early endosome triggers retrograde motility. The dynein comet was therefore considered to be a “loading zone” for early endosomes (Lenz et al. 2006).

1.7 Conclusions and objectives

Hyphal growth of *U. maydis* is essential for infection of plants. The formation of the elongated hyphal cells requires long-distance transport of organelles along the cytoskeleton (Schuchardt et al., 2005). Among these are the early endosomes, which move in a bidirectional fashion along microtubules. The motors that support this transport are kinesin-3 and dynein, and dynein is delivered to microtubule plus-ends by the motor kinesin-1. How these motors cooperate in bidirectional trafficking is not well understood. It was the goal of this work to analysetheir precise role in early endosome motility and to increase our understanding of motor cooperation in this process. Using live cell imaging techniques, including photo-activation, photo-bleaching of fluorescent proteins and quantitative fluorescence microscopy in the dimorphic fungus *U. maydis,* I addressed three aspects of bidirectional early endosome trafficking. Firstly, I analysed the function of the dynein accumulation at the microtubule plus ends. In the second part of this thesis, I present a detailed analysis of the way kinesin-3 and dynein cooperate in early endosome motility. In the a third part, I include the organization of the microtubule cytoskeleton and consider the implication of a bipolar microtubule array in bidirectional endosome motility. The outcome of the first and the second part of my work was recently published, and the third chapter has been submitted for publication and is in the moment under revision.

Chapter 2
The mechanism of organelle capture at the end of a microtubule

Early endosomes get loaded onto dynein at the plus ends of microtubules (Ligon et al., 2003, Lenz et al., 2006, Abenza et al., 2009). It was reported that an accumulation of dynein at the microtubule end is involved in the capture of endosomes (Lenz et al., 2006). Here I present the results of a study that addresses the organization, dynamics and function of this "dynein comet". I show that ~55 dynein motors are concentrated in a single comet and that this high number is achieved by a stochastic accumulation and an active retention mechanism. This dual mechanism ensures that an excess of dynein motors is provided which increases the possibility that an arriving early endosome gets captured by the retrograde transport machinery. This prevents the organelles from "falling off" their track and ensures continuous bidirectional motility.

This work was built on previous work and was undertaken with the help of co-workers. Prof. Nicholas Severs provided the freeze-fracture electron microscopy data that serve as a control, showing nuclear pores being single units in the nuclear envelope of *U. maydis*. Dr. Sreedhar Kilaru provided plasmids and strains in which nuclear pore proteins were labelled, and which were used to establish nuclear pores as an internal calibration standard to estimate the number of GFP molecules from fluorescence intensity. In addition, he designed and generated the inhibitory plasmids used to demonstrate that the interaction of the $p150^{glued}$ dynactin subunit and EB1 anchors dynein at microtubule plus-ends. All mathematical modelling and the non-linear regression analysis were provided by Ms. Congping Lin and Prof. Peter Ashwin from the Department of Mathematics in Exeter. They found theoretical evidence for a stochastic mechanism that concentrates half of the dynein motors in the comet. Prof. Gero Steinberg provided overall project management and supervision, analyzed data and wrote the manuscript. The data presented in this chapter were recently published in 2011 in the EMBO Journal 30, 652–664.

This Chapter has been removed by the author of this thesis for copyright reasons. The paper can be found on the publisher home page:

http://www.nature.com/emboj/journal/v30/n4/full/emboj2010360a.html
http://www.nature.com/emboj/journal/v30/n4/suppinfo/emboj2010360as1.html

Chapter 3
Dynein controls bidirectional motility of early endosomes by transient binding to the organelle

It was previously reported that kinesin-3 and cytoplasmic dynein mediate bidirectional motility of early endosomes in the fungus *Ustilago maydis* (Wedlich-Söldner et al., 2002a, Lenz et al., 2006). The following chapter summarises results that describe the precise mechanism by which dynein and kinesin-3 cooperate in this process. Using live-cell imaging of native levels of fluorescent motors, I was able to show that Kinesin-3 always localizes on early endosomes, whereas dynein is only transiently found on retrograde organelles. Binding of moving dynein to anterograde moving early endosomes changes their transport direction. An analysis of motor numbers by using quantitative photo-bleaching and comparison with nuclear pores as an internal calibration standard revealed that single dynein motors counteract three to five kinesin-3 motors in organelle motility. When dynein leaves the organelle, kinesin-3 can take over again and takes the early endosomes in anterograde direction. These data imply that dynein binding and unbinding limits the activity of kinesin-3 and thereby controls bidirectional long-range motility of the early endosomes.

This work was built on previous work and was undertaken with the help of co-workers. Prof. Reinhard Lipowsky from the Max-Planck Institute in Golm, Germany, discussed the results and analysed some data. Mr. Marcus-Alexander Assmann and Prof. Peter Lenz from the Department of Physics, University of Marburg, Germany, developed a mathematical model that added support to the experimentally described mechanism of dynein controlling early endosome motility. Prof. Gero Steinberg provided overall project management and supervision, analyzed data and wrote the manuscript. The data presented in this chapter are published in 2011 in PNAS 108, 3618-3623.

This Chapter has been removed by the author of this thesis for copyright reasons. The paper can be found on the publisher home page:

http://www.pnas.org/content/108/9/3618.long
http://www.pnas.org/content/108/9/3618/suppl/DCSupplemental

Chapter 4
Kinesin-3 mediates long-distance anterograde and retrograde endosome motility

Hyphal cells of *U. maydis* contain anti-polar microtubules in their mid region The microtubules extend their plus-ends towards both cell poles. In animal dendrites, an anti-polar microtubule array allows the cell to evenly distribute vesicles and organelles using dynein. In this chapter I summarise results which demonstrate that the bi-polar microtubule array in *U. maydis* determines the use of motors in long-range motility of early endosomes. Visualising early endosome motility in temperature-sensitive dynein and kinesin-3 mutants revealed that long-range endosome motility starts at one cell pole as minus-end directed motion. At the transition from the uni-polar to the bi-polar microtubule array kinesin-3 takes over and continues the backward motility of the organelles towards microtubule plus ends within anti-polar microtubule bundles. Dynein is only essential for the first 10-20 micrometers of retrograde motility. Thus, both motors cooperate to support the same transport direction.

This work was built on previous work and was undertaken with the help of co-workers. Dr. Sreedhar Kilaru generated the fast-reacting temperature-sensitive kinesin-3 mutant strain. Ms Yvonne Roger analyzed data and provided the kinesin-3/dynein double mutant to show that motility is exclusively based on these two motors. Dr. Jerome Collemare visualized the long-range motility of photo-activatable GFP-Rab5a on early endosomes and analyzed the co-localization of kinesin-3-GFP with retrograde moving organelles. Dr. Gero Fink has analyzed the MT-bundling. Prof. Gero Steinberg provided overall project management and supervision, analyzed data and wrote the manuscript. The data presented in this chapter are submitted to the EMBO Journal.

Kinesin-3 and dynein cooperate in long-range retrograde endosome motility along a non-uniform microtubule array

Martin Schuster[1], Sreedhar Kilaru[1], Gero Fink[2], Jérôme Collemare[3], Yvonne Roger[1] and Gero Steinberg[1,4]

[1] Department of Biosciences, University of Exeter, Exeter EX4 4QD, UK

[2] Max Planck Institute of Molecular Cell Biology and Genetics, D-01307 Dresden, Germany

[3] present address: Laboratory of Phytopathology, Wageningen University, 6708 PB Wageningen, The Netherlands

[4] To whom correspondence should be addressed: G.Steinberg@exeter.ac.uk; phone: ++44-1392-263476; fax: ++44-1392-263434;

Word count: 49324 characters, Main Text, Abstract, Methods, Figure legends; Abstract has 232 words

Subject category: Membranes and Transport

Abbreviations: Microtubule, MT; enhanced green-fluorescent protein, eGFP; mRFP, monomeric red-fluorescent protein; early endosomes, EEs

Abstract

The polarity of microtubules determines the motor system for intracellular motility, with kinesins moving to plus-ends and dynein transporting to minus-ends. In the elongated cells of the filamentous fungus *Ustilago maydis* dynein is thought to be the motor for backward (=retrograde) motility of early endosomes (EEs), whereas kinesin-3 is the anterograde (=forward) transporter, delivering the organelles to the plus-ends at the growing cell tip. Here we show that kinesin-3 is also the main motor for long-range retrograde EE motility. Using photo-activatable GFP-Rab5 we demonstrate that single EEs travel for up to 90 µm. This motility occurs along a dendrite-like microtubule array, with uni-polar microtubules at the distal cell ends but anti-polar orientation along most of the cell body. Long-range EE runs start minus-end directed, but later switch to plus-end directed, suggesting that both dynein and kinesin-3 are involved. Indeed, inactivation of a temperature-sensitive dynein abolished motility along the uni-polar microtubule array, but did not affect long-range retrograde EE motility along the anti-polar microtubule array. Consistently, dynein co-localizes with EEs only for the initial 10-20 µm. In contrast, kinesin-3 is continuously present on retrograde EEs and its activity is essential for long-range retrograde motility. This indicates that dynein is supporting the initial short-range retrograde motility, whereas kinesin-3 is the motor for long-range EE transport along the bi-polar microtubule array. The cooperation of both motors mediates EE motility that connects both cell ends.

INTRODUCTION

Long-range organelle transport organizes eukaryotic cells and enables communication over large distances. The importance of long-range motility is illustrated by the fact that numerous neuronal diseases are related to defects in axonal transport (Chevalier-Larsen & Holzbaur, 2006; Duncan & Goldstein, 2006). Long-range intracellular membrane trafficking utilizes microtubules (MTs) and is driven by molecular motors kinesin and dynein (Hirokawa & Takemura, 2004; Vale, 2003). MTs are tubulin-polymers that expose beta-tubulin at their more dynamic plus-end (Nogales et al, 1999). Motors recognize this intrinsic polarity, with kinesins generally moving to the plus-ends and dynein travelling to the minus-ends (Vale, 2003). Both motor systems often oppose each other, thereby mediating bi-directional organelle transport (Ally et al, 2009; Gross, 2004; Müller et al, 2008; Welte, 2004). How motors cooperate is under intensive investigation. Currently, most concepts consider a scenario in which both motors counteract while being bound to the same organelle. Here they seem to coordinate their activity in a tug-of-war (Hendricks et al, 2010; Müller et al, 2008; Soppina et al, 2009), often in conjunction with higher order control by regulatory factors (Deacon et al, 2005; Deacon et al, 2003; Gross et al, 2002a; Larsen et al, 2008; Welte et al, 2005; Welte et al, 1998). This leads to bi-directional cargo motion, with individual runs normally spanning a few micrometers (Shubeita et al, 2008; Soppina et al, 2009; Welte et al, 1998).

In elongated neurons and filamentous fungi, organelle transport can be very persistent, with individual runs extending over 35 µm and more (Abenza et al, 2009; Barkus et al, 2008; Higuchi et al, 2006; Lee et al, 2003; Smith et al. 2004). In *Drosophila melanogaster*, the motor for such long-range forward

motion (=anterograde) to the growth cone is kinesin-3, whereas dynein is responsible for backward (=retrograde) transport (Barkus et al, 2008; Pilling et al, 2006). Interestingly, mutations in kinesin-3 inhibit both anterograde and retrograde organelle motility (Barkus et al, 2008). It is not known by which way defects in kinesin-3 affect retrograde membrane trafficking. One possibility is that kinesin-3 and dynein bind to the same organelle and that the presence of kinesin-3 activity is required for dynein-based motility. Such a scenario was recently described for peroxisomal movements (Ally et al, 2009). Indeed, kinesin-3 localizes to dynein-driven organelles (Koushika et al, 2004) and fluorescent kinesin-3-GFP travels bi-directionally in mammalian, worm and insect neurons (Barkus et al, 2008; Lee et al, 2003; Zhou et al, 2001). However, another option is that the orientation of the underlying MT array supports retrograde kinesin-3 motility. Neuronal dendrites contain anti-polar MT bundles (Baas, 1999; Baas et al, 1988). It is therefore conceivable that bi-directional motility could reflect kinesin-3-based organelle transport along such a bi-polar MT array (Zhou et al, 2001).

The fungus *Ustilago maydis is* a genetically tractable model system for long-range membrane trafficking (Steinberg & Perez-Martin, 2008). This organism forms elongated hyphal cells of ~80-100 µm length that grow at the cell tip and form a septum at the rear cell end. Early endosomes (EE) move processively over >20 µm towards the hyphal tip (=anterograde; Schuster et al. 2011a) and backwards towards the septum (=retrograde). The biological function of this transport is not known, but it was speculated that retrograde EE motility mediates communication between the hyphal tip and the nucleus (Steinberg, 2007), which is positioned in the middle of the cell. The elongated

hyphal cells of *U. maydis* contain long MTs (Steinberg et al, 2001) that form an anti-polar MT array with plus-ends being directed to both cell poles (Lenz et al, 2006). Long-range EE motility occurs along MTs (Wedlich-Söldner et al, 2000), and is mediated by kinesin-3 and dynein (Lenz et al, 2006; Wedlich-Söldner et al, 2002a). In dynein mutants, the EEs are trapped near the apical plus-ends, suggesting that dynein supports retrograde EE motility (Lenz et al, 2006). Indeed, live cell imaging of native levels of motors and EEs revealed that dynein binds to retrograde EEs (Schuster et al, 2011a). Similar to animal neurons, kinesin-3 supports motility towards the expanding cell end (Lenz et al., 2006) and it consequently locates to anterograde EEs (Schuster et al. 2011a). Kinesin-3 is also bound to retrograde organelles (Schuster et al, 2011a), which might support recycling of inactive kinesin-3. Here we show that anti-polar MT bundles occupy most of the hyphal cell and that kinesin-3 has an active role on retrograde EEs. By taking over from dynein at the barrier between uni-polar MT to anti-polar MT bundles, kinesin-3 supports long-range motility of EEs.

RESULTS

Hyphal cells contain an extended anti-polar array of MT bundles

Under laboratory conditions, the fungus *U. maydis* forms elongated hyphal cells that expanded at the growing cell tip and form sub-apical septa at the rear cell pole, whereas the nucleus is positioned near the cell center (Figure 1A). It was previously reported that the plus-ends of the MTs, labeled by the EB1-homologe Peb1 fused to the yellow fluorescent protein (Peb1-YFP; Straube et al, 2003), are directed towards the growing tip (Schuchardt et al, 2005), but form an anti-polar array near the cell center (Lenz et al, 2006). We performed a more detailed study, using Pep1-YFP and GFP-α-tubulin, and determined the

orientation of MTs along the length of the cell and the degree of MT bundling. Within the first 10 µm behind the growing tip or the rear septum >96% of the MT plus-ends elongate towards the cell poles, forming regions of uni-polar MT orientation at both cell ends (Figure 1B, 1C; Supplementary Movie S1). Towards the middle part of the cell, the orientation of the MTs changed, resulting in a non-uniform MT array that occupies ~70% of the cell length (Figure 1C). Here, the cells contained on average 2.0±0.7 (n=26) continuous MT tracks, labeled with green-fluorescent protein fused to alpha-tubulin (GFP-Tub1; Steinberg et al, 2001). In order to test if these MT tracks represent multiple MTs we performed a fluorescence intensity analysis. We found that the fluorescence intensity of these tracks was stronger in the cell center than towards the cell poles (Figure 1D, compare section 1 and 4; 3D-reconstruction from Z-axis stacks; Movie S2). Such increase in intensity reflects a higher number of MTs in a MT bundle (Straube et al, 2006), suggesting that MTs have strong tendency to form bundles in this part of the hyphal cell. MTs of weaker intensity disappeared when depolymerizing, suggesting that they are unbundled tubulin polymers. We measured the signal intensity in MT tracks and compared it to the signal intensity of single and unbundled MTs. From this we estimated that most tracks consist of 2-4 MTs, which was in the range of MT bundling in yeast-like cells of *Ustilago maydis* (Straube et al, 2006). Single MTs were mainly found near the cell ends, whereas almost all MTs were bundled in the central cell region (Figure 1E; only one half of the cell is shown). To see whether these MT bundles contain uni- or anti-polar oriented MTs, we co-expressed Peb1 fused to monomeric red fluorescent protein (mRFP) and GFP-Tub1. In bundles located in the central part of the cell, Peb1-mRFP signals move away from each other (Figure 1F). This suggests that they are composed

of anti-polar MTs. Near the cell ends MT bundles were seen, in which Peb1-RFP signals moved in the same direction (Figure 1G), suggesting that they consist of uni-polar MT bundles. Taken together, hyphal cells contain a symmetric, bi-polar MT array of uni-polar MT bundles close to the cell poles and anti-polar bundles throughout the cell centre.

Motility of early endosomes across the bi-polar MT array is symmetric

In *U. maydis* cells, EEs rapidly move in a bi-directional fashion (Wedlich-Söldner et al, 2000). Their large number, however, makes it very difficult to follow individual organelles over longer distances. To avoid interferences between EEs we visualized single organelles by expressing a fusion protein of photo-activatable paGFP fused to the endosomal GTPase Rab5a (Schuster et al, 2011b). When activated by a 405 nm laser pulse at the hyphal tip (Figure 2A, arrowhead), occasionally single EEs became visible that continuously travel in retrograde direction (Figure 2A; Movie S3). Interestingly, all retrograde organelles paused shortly after they left the tip (Figure 2A, inset). Most EEs paused once for less than 0.6 s (Figure 2B, 2C), and this occurred ~10-20 µm behind the cell tip (Figure 2D), which coincides with a change in MT bundle orientation from uni-polar to anti-polar (see above). The majority of the organelles turned back to anterograde motility within the first 50 µm (Figure 2E, light blue bars). However, some EEs traveled over longer distances and reached into the region of uni-polar MT orientation at the rear cell pole where the septum is formed (Figure 2A; Movie S3). This indicates that these organelles begin their retrograde runs at the hyphal tip with minus-end directed motility, but eventually switch to plus-end directed motility to reach MT plus-ends at the rear cell pole, where they turned direction again and moved back

towards the cell center (Figure 2A). Similar behavior was observed for EEs leaving the MT plus-ends at the septum.

The similarity in the motility behavior of EEs coming from opposite poles and the symmetric bi-polar organization of the MT array suggested that the underlying transport mechanism might be the same for both directions. It was shown that retrograde EE motility involves dynein that is released from a comet-like accumulation at MT plus-ends (Lenz et al, 2006; Schuster et al, 2011b). Consistent with the symmetry of the MT array, we found such dynein comets at MT plus-ends at both poles of the cell (Figure 3A). From here, dynein leaves to travel towards the cell center (Figure 3B). Thus, bi-directional EE transport is a balanced process with motility towards the cell middle being most likely supported by dynein. However, some EEs travel from one to the other cell pole using the entire bi-polar MT array. This suggested that their motility involves dynein and kinesin-3.

Dynein supports short range retrograde EE motility

In *U. maydis* cytoplasmic dynein supports minus-end-directed EE transport (Lenz et al, 2006; Wedlich-Söldner et al, 2002a) and it is able to travel over long distances (Schuster et al, 2011a). To investigate whether dynein plays a role in the long-range retrograde transport of EEs, we observed GFP-Rab5a in mutants containing a temperature-sensitive dynein allele (*dyn2*^{ts}; Wedlich-Söldner et al, 2002b). This allowed the observation of EE motility in the absence of functional dynein before a steady state is reached when the organelles are trapped at plus-ends due to the unbalanced activity of kinesin-3 (Lenz et al. 2006). At permissive temperature (22°C), EEs showed bi-directional motility

(Figure S1). When hyphal cells were shifted to restrictive conditions for 30 minutes, EEs started to accumulate at plus-ends near the hyphal tip (asterisk in Figure 4A, Movie S4). This apical clustering is most likely due to kinesin-3 that moves EEs to the MTs plus-ends, where they are trapped due to the absence of functional dynein (Lenz et al, 2006). No retrograde motility was found in the apical ~10 µm (average: 9.63±2.88, *n*=30; Figure 4A and 4B, Movie S4), suggesting that dynein is not functional and therefore cannot overcome the uni-polar MT array near the cell ends. The lack of motility was not due to the absence of the tracks, as MTs were even longer in *dyn2*^{ts} mutant hyphae and reached into the hyphal apex (Figure 4C). However, those EEs that have not yet become trapped at plus-ends still travel over long distances in the central part of the cell (Figure 4A, arrowheads; Figure 4D; Movie S4) and their run-length was even slightly enhanced by the inactivation of dynein (Figure 4D; different to control; Mann-Whitney Test, *P*=0.013).These results suggest that dynein is crucial for short-range retrograde motility within the uni-polar MT array near the hyphal tip, whereas sub-apical long-range EE motility does not require dynein.

It was previously shown that single dynein motors co-localize with retrograde EEs near the cell tip (Schuster et al, 2011a). To understand the role of dynein in long-range motility in sub-apical regions, we simultaneously observed mCherry-Rab5a and G_3Dyn2 in more sub-apical regions of control hyphae. In agreement with a role of dynein in the distal part of the hyphal cell, we found the previously reported high degree of co-localization in the first 10 µm (Figure 5A). In more sub-apical regions, however, an increasing number of dynein signals lost their co-localizing with EEs (Figure 5A; supplementary Movie

S5). Binding and unbinding of dynein to EEs was reported to change in transport direction in the apical region of the cell (Schuster et al, 2011a). We found such cases also in the sub-apical parts of the hyphal cell (Figure 5B; spatial position relative to the cell apex is indicated in lower left corner of the kymograph). However, we also observed that dynein unbinds from EEs, but after a brief pause the organelles continued traveling in retrograde direction (Figure 5C). The short pauses were mainly found at ~10-20 µm behind the tip, which corresponds to the brief pausing in retrograde EE motility, described above (see Figure 2A, inset). This raises the possibility that this irregularity in the retrograde transport marks the point when dynein unbinds from the EE. Taken together these results suggest that dynein supports motility along the uni-polar parts of the MT array near the cell poles, whereas another motor supports retrograde motility within the bi-polar array.

Kinesin-3 is required for long-range retrograde endosome transport

In yeast-like cells of *U. maydis* EEs are transported solely by kinesin-3 and dynein (Wedlich-Söldner et al, 2002a). To confirm that kinesin-3 and dynein are the only motors driving EE transport in the elongated hyphal cells, we replaced the promoter of dynein by the conditional *crg* promoter (Bottin et al, 1996) in a kinesin-3 null mutant. When dynein was depleted in these mutant cells, EEs often clustered and almost no EE motility was seen (Figure 6A; Movie S6). This strongly indicates that EE motility in hyphal cells is solely mediated by kinesin-3 and dynein. As a consequence, we considered it likely that the retrograde EE motility in dynein mutants is mediated by kinesin-3. Indeed, kinesin-3 co-

localized with retrograde EEs in all parts of the hyphal cell (Figure 6B, 6C) and traveled over long distances in retrograde direction (Movie S7).

To test whether kinesin-3 has an active role in retrograde EE motility, we aimed to interfere with kinesin-3 activity and to investigate the effect on EE motility. Existing conditional or deletion mutants did not form proper hyphae (Lenz et al, 2006) and, consequently, did not allow the investigation of the long-range transport of EEs along a symmetric bi-polar MT array. We therefore generated a "fast-reacting" temperature-sensitive kinesin-3 allele (*kin3*^{ts}) in which kinesin-3 activity was abolished after shifting proper hyphal cells for a few minutes to restrictive temperature (see Material and Methods for details). At permissive temperature (22°C), *kin3*^{ts} mutant strain formed long hyphal cells and normal bi-directional motility of EEs was found (Figure 6D, 22°C). After 5 minutes at restrictive temperature (32°C), motility was severely impaired (Figure 6D, 32°C; Movie S8) and EE began to cluster, which was most prominent at 10-20 µm behind the tip (average: 12.43±3.25 µm, n=25; Figure 6D, 32°C, asterisk). This supports the notion that kinesin-3 is taking over from dynein at central anti-polar MT bundles. Motility was severely impaired and in most cells EEs did not reach beyond the middle region of the cell (arrow, Figure 6D, 32°C; Movie S8). With time at restrictive conditions, the motility further decreased and clusters of EEs were found in the middle region of the cell (Figure S2). Some motility was still present, which could be residual activity of Kin3^{ts} or due to dynein which might bind and subsequently move stationary EEs.

In insect cells, motor activity of kinesin is required to enable dynein-based motility (Ally et al, 2009). This raised the possibility that the defect in EE

motility is due to impaired dynein activity in the kinesin-3^{ts} mutants. To test this we visualized the temperature-sensitive Kin3^{ts}-GFP motor on EEs at restrictive and permissive temperature. At permissive Kin3^{ts}-GFP and mCherry-Rab5a co-localized (Figure 7A). At restrictive temperature the inactivated motor remained bound to the organelles (Figure 7B; Movie S8), suggesting that the temperature-sensitive mutations did not affect the attachment to the EEs, but rather impaired the motor activity of Kin3^{ts}. To see whether the inactive motor inhibits dynein activity, we analyzed the motility of dynein, labeled with triple-GFP fused to its endogenous heavy chain (Schuster et al, 2011b), in *kin3*^{ts} mutants. We found that the inactivation of Kin3^{ts} showed no effect on dynein motility (Figure 7C). This result confirms previous findings that dynein leaves the plus-end of MTs in Kin3^{rigor} mutants, where the mutated kinesin-3 motor was tightly anchored to the MTs (Schuster et al, 2011b). Taken together these results strongly argue for kinesin-3 being the main motor to transport EE across a non-uniform MT array.

DISCUSSION

Kinesin-3 and dynein participate in retrograde EE motility

It was previously reported that when dynein is inactivated in *U. maydis*, kinesin-3 takes over and shifts EEs to the plus-ends (Lenz et al, 2006). On the other hand, depletion of kinesin-3 results in the concentration of the EEs at minus-ends near the cell center (Lenz et al, 2006). Thus, it was concluded that kinesin-3 is the transporter for anterograde motility to the tip, whereas dynein mediates retrograde organelle transport towards the cell center (Lenz et al, 2006). Using fast-reacting temperature-sensitive mutants we show here that dynein is essential for retrograde motility along uni-polar MT bundles at the cell ends, but

that kinesin-3 is the major motor for retrograde EE motility reaching toward the cell centre. Dynein and kinesin motors are usually found on the same organelle (Gross et al, 2002b; Hirokawa et al, 1990; Rogers et al, 1997; Ligon et al, 2004; Pedersen et al, 2006), where they counteract each other in a tug-of-war (Hendricks et al, 2010; Müller et al, 2008; Soppina et al, 2009) or control each others activity by physical interaction or binding to a common regulator (Deacon et al, 2005; Guillaud et al, 2008; Larsen et al, 2008; Welte et al, 2005; Welte et al, 1998). In *U. maydis* kinesin-3 is always bound to the EEs, whereas dynein is released from a comet-like accumulation (Schuster et al. 2011a, b). When dynein meets an anterograde EE it can bind the organelle, which changes the transport direction from anterograde to retrograde. It was reported that unbinding of dynein results in rebinding of kinesin-3, which in results in a switch to anterograde motility towards the plus-end at the hyphal tip (Schuster et al, 2011a). In the distal parts of the cell, where MTs are uni-polar, this is the most likely scenario. However, our data suggest that in the sub-apical region, where MTs form anti-polar bundles, rebinding of kinesin-3 maintains the initial transport direction. This is most likely due to the ability of kinesin-3 to interact with MTs of opposite orientation (Figure 8). The organization of the MTs in anti-polar bundles is probably supporting this mechanism. In yeast-like cells of *U. maydis* the individual MTs within a bundle are only ~10 nm apart (Straube et al., 2006). It therefore seems likely that the 3-5 kinesin-3 motors on a dynein-driven EE (Schuster et al., 2011a) can bind to the adjacent MT within the bundle, when the bi-polar array begins. Unless this kinesin-3-driven EE meets a dynein that is released from the plus-ends at the rear cell pole, it can continue moving towards the septum. There it finally reaches the end of the MT array, where dynein is concentrated in comets to ensure efficient loading onto dynein, which

prevents EEs falling off the track (Schuster et al, 2011b). Thus, the symmetric organization of the MT array ensures bi-directional and long range motility that is mainly based on the activity of kinesin-3.

A bi-polar microtubule array allows extended motility of early endosomes

In this study we show that EEs can processively move for up to 90 µm from the hyphal tip all the way back to the septum. Long distance motility of organelles was reported in other elongated cells (Barkus et al, 2008; Koonce & Schliwa, 1986; Miller et al, 2005; Smith et al, 2004). While single motors are able to move an organelle (Shubeita et al, 2008; Soppina et al, 2009; Schuster et al, 2011a), *in vitro* data indicate that single motors can only travel over one to a few micrometers (Howard et al, 1989; Reck-Peterson et al, 2006; Thorn et al, 2000; Wang et al, 1995). However, when several motors of the same kind cooperate on the cargo, much larger distances can be overcome (Klumpp & Lipowsky, 2005; Mallik et al, 2005). We recently demonstrated that 2-5 kinesin-3 motors are bound to EEs in *U. maydis* and have theoretically estimated that 4 motors are sufficient to overcome ~97 µm (Schuster et al, 2011a). These results are in agreement with our conclusion that the non-uniform bi-polar MT array allows several kinesin-3 motors to travel EEs over the entire length of the cell.

The most pressing question is why EEs travel over such long distances. In neurons, retrograde motility of EEs is involved in neurotrophic signalling between the distal synapsis and the cell body (Delcroix et al, 2003; Howe & Mobley, 2005; Miaczynska et al, 2004). By this mechanism, the nucleus receives information from the distal cell end. In *U. maydis* the nucleus is positioned 40-50 µm behind the expanding tip and maintains this position while

the cell expands. In analogy to retrograde signalling in neurons, it has been speculated that retrograde EE motility supports communication between the cell tip and the nucleus (Steinberg, 2007). However, such a role of EEs does not explain the extended pole-to-pole runs by which EEs connect the tip and the septum. Long-range motility of EEs might serve another signalling aspect. When hyphal cells of *U. maydis* continuously expand at the growing tip, they simultaneously form septa at the rear cell end to move their cytoplasm forward (Steinberg et al, 1998). This suggests that septum formation and tip advancement must be synchronised. We speculate that EEs provide means to communicate between both cell ends by random long-range walks along the anti-polar MT array. While such a function of long-range motility of EEs in signalling is tempting, it need to be emphasized that experimental evidence for such a role is currently missing.

U. maydis cells contain a non-uniform microtubule array similar to dendrites

The surprising outcome of this study is that kinesin-3 is the major motor for retrograde EE motility. In contrast, in axons the major motors for retrograde EE motility is cytoplasmic dynein (Ha et al., 2008), which moves its cargo from the expanding growth cone back to the cell center (Hirokawa & Takemura, 2004; Vale, 2003). This difference is most likely due to the discussed differences in the orientation of the MTs arrays. In neurons the axonal MT array is uniform with the plus-ends facing towards the growth cone (Burton & Paige, 1981; Heidemann et al, 1981). Consequently, retrograde transport is based on the minus-end directed motor dynein. In contrast, dendrites contain a non-uniform bi-polar MT array with uni-polar regions at the tip of the dendrite (Baas et al,

1988; Baas et al, 1991). The latter corresponds well with the overall organization in *U. maydis* cells, and the presence of an extended anti-polar MT array allows kinesin-3 to support long-range retrograde EE motility.

In neurons, it is thought that the differences in MT organization are responsible for neuronal polarity and the structural differences between axons and dendrites (Baas et al, 1988; Baas & Lin, 2010; Black & Baas, 1989). This is done by selective recruitment of motors which allows dynein to transport Golgi membranes into dendrites, but not axons (Baas & Lin, 2010; Zheng et al, 2008). It was speculated that a similar mechanism accounts for the presence ribosomes in the dendrite (Baas and Lin, 2010). In fungi ribosomes are concentrated at the growing tip (Howard, 1981; Howard & Aist, 1979), and similar to dendrites Golgi membranes in *U. maydis* are distributed along the hyphal cell, with a gradient towards the hyphal tip (Steinberg & Schuster, 2011; Wedlich-Söldner et al, 2002b). The mechanism of ribosome and Golgi positioning in *U. maydis* is not known. However, if the situation is similar to dendrites, the anti-polar MT array could help dynein to position ribosomes and Golgi vesicles. Thus, the need to distribute the organelles by minus-end motors might have dictated the organization of the MT array.

Conclusion

Bi-directional organelle transport is a characteristic feature of eukaryotic cells (Gross, 2004; Welte, 2004). The way by which motors cooperate on a single organelle is under intensive investigation (Ally et al, 2009; Gross et al, 2002a; Hendricks et al, 2010; Müller et al, 2008). However, the cellular use of motors in organelle motility depends on the organization of the underlying MT array. In

neurons differences in the orientation of MTs are of functional importance for axons and dendrites (Baas & Lin, 2010), and the bi-polar MT array in dendrites supports a dynein-based cargo sorting mechanism (Kapitein et al, 2010; Zheng et al, 2008). Hyphal cells of *U. maydis* also contain a similar non-uniform bi-polar microtubule array. This array is the basis for symmetric organisation of the cell. Dynein accumulates at both ends of the array, from where it is released and stochastically interacts with kinesin-3-delivered EEs to turn their transport direction (Schuster et al. 2011a, 2011b). We show here that the combined activity of dynein and kinesin-3 enables individual organelles to run over the entire bi-polar MT array. This might support long-range communication between both cell ends, thereby synchronising cell expansion and septum formation. Moreover, the organization of the MT array might allow organelle positioning by a single motor. In dendrites, bi-directional motility of dynein supports stable distribution of vesicles in dendrites (Kapitein et al., 2010). In *U. maydis* many organelles, including mitochondria, peroxisomes, Golgi membranes and the endoplasmic reticulum are distributed along the hyphal cell (Steinberg & Schuster, 2011). Dynein was shown to mediate motility within the endoplasmic reticulum (Wedlich-Söldner et al, 2002b) and the bi-polar array would support a more general role of dynein in organelle distribution. Thus, the use of a symmetric and anti-polar MT array in *U. maydis* offers a maximum of flexibility, allowing an efficient organization of the elongated cell with a minimum set of molecular motors.

Material and Methods

Strains and plasmids

The *Ustilago maydis* strains AB33nRFP, AB33paGRab5a, AB33GT_Peb1R, AB33G_3Dyn2, and AB33G_3Dyn2_ChRab5a were described previously (Lenz et al, 2006; Schuchardt et al, 2005; Schuster et al, 2011a; Schuster et al, 2011b). The orientation of MT was investigated in strain AB33EB1Y, which was generated by homologous integration of plasmid pPeb1Y_N (Lenz et al, 2006) into strain AB33. In order to analyze MT bundles, plasmid potefGFPTub1 (Steinberg et al, 2001) was ectopically introduced into strain AB33 resulting in AB33GT. The strain AB33GT_Peb1R was obtained by homologous integration of plasmid pPeb1R_N (Lenz et al, 2006) into AB33GT. The strain AB5Dyn2^{ts}_GT was generated by ectopic integration of plasmid potefGFPTub1 in the strain AB5Dyn2^{ts}. For co-localisation studies of dynein and MT, plasmid potefGFPTub1 was ectopically integrated into strain AB33G_3Dyn2 resulting in AB33G_3Dyn2_GT. For strain AB33_ΔKin3_r Dyn1_GRab5a the phleomycin resistance cassette of plasmid pcrgDyn1 (Lenz et al, 2006) was replaced by the hygromycin resistance cassette resulting in plasmid pcrgDyn1-H. This plasmid was transformed in strain AB33_ΔKin3_GRab5a. potagRRab5a was generated by replacing the paGFP in plasmid popaGRab5a (Schuster et al. 2011b) with TagRFP (Evrogen, Moscow, Russia). The resulting plasmid potagRRab5a was linearized with *Age*I for homologous integration at the succinate dehydrogenase locus of strain AB33ΔKin3_Kin3^{ts}G resulting in AB33ΔKin3_ Kin3^{ts}G_tagRRab5a.

To visualize kinesin-3-GFP, a 1036 bp fragment near the 3-prime end of the gene followed by *egfp* and the *nos* terminator, the hygromycin resistance cassette and 1032 bp of the downstream sequence were cloned into a cloning

vector resulting in plasmid pKin3G_H. The plasmid was integrated into the native kin3 locus resulting in strain AB33Kin3G. All strains and plasmids used in this study are summarized in Table 1.

Generation of a temperature-sensitive *kinesin-3* mutant

To generate the temperature-sensitive mutants in *kin3*, error prone PCR approach was used (modified from (Spee et al, 1993). The *kin3* gene was cloned behind its own promoter and followed by the terminator sequences into a self-replicating plasmid, resulting in plasmid pNEBUH-Kin3. Primers were designed to PCR-amplify 4 fragments that partially overlapped and covered the entire ORF of *kin3.* Each primer pair was used in 8 PCR reactions, each using 80 or 90% short fall of one of the 4 dNTP. The products from these 32 PCR reactions were pooled and together with the linearized plasmid pNEBUH-Kin3, lacking the *kin3* ORF, was transformed into the yeast *Saccharomyces cerevisiae* for *in vivo* recombination (further details are described in (Schuster et al, 2011b). The resulting plasmid pool was obtained from yeast and amplified in *E. coli*. After recovery, the plasmid pool was transformed into strain AB33ΔKin3 following published procedures (Schulz et al, 1990). Transformed cells were replica plated from transformation plates, where they grow as yeast-like cells without phenotype, onto hyphal growth-inducing nitrate minimal plates, supplemented with 1% glucose (Brachmann et al, 2001). After cells were incubated at 22°C and 32°C for 3 days and restoring of hyphal growth at low temperature, but not at high temperature was monitored. 15 positive colonies were collected; their self-replicating pNEBUH vectors carrying mutated $kin3^{ts}$ genes were isolated and transformed into strain AB33ΔKin3_GRab5a. EE motility was analysed in all strains at 22°C and 32°C and one strain was

selected that showed normal motility at 22°C, but almost no motility of EEs after 5 minutes at 32°C. This *kin3^{ts}* allele was ectopically integrated into strains AB33ΔKin3_G_3Dyn2 and AB33ΔKin3_paGFP-Rab5a, respectively, resulting in AB33ΔKin3_Kin3^{ts}_G3Dyn2 and AB33ΔKin3_Kin3^{ts} _paGFP-Rab5a. The plasmid pKin3^{ts}G was generated through *in vivo* recombination in the yeast *S. cerevisiae* by cloning PCR amplified fragment of *egfp-GFP-Tnos* (1016 bp) with 30 bp overhang sequences into *Bsr*GI digested plasmid pKin3^{ts}. The resulting plasmid pKin3^{ts}-G was digested with *Psi*I and *Hpa*I and transformed in to AB33ΔKin3 resulting in AB33ΔKin3_Kin3^{ts}G.

Growth conditions

All cultures of *U. maydis*, with the exception of kinesin-3 and dynein temperature sensitive strains, were grown overnight at 28ºC in complete medium (CM, Holliday, 1974) containing 1% (w/v) glucose, shaking at 200 revolutions per minute (rpm). Hyphal growth was induced by shifting in NM liquid medium supplemented with 1% (w/v) glucose (Brachmann et al, 2001). The strains AB33ΔKin3_Kin3^{ts}_GRab5a, AB33ΔKin3_Kin3^{ts}_paGRab5a, AB33ΔKin3_Kin3^{ts}_G_3Dyn2, AB33ΔKin3_Kin3^{ts}G_tagRRab5a, AB5Dyn2^{ts}_GRab5a and AB5Dyn2^{ts}_GT were grown for 10h at 22ºC in complete medium (CM) containing 1% (w/v) glucose, shaking at 200 revolutions per minute (rpm). Hyphal growth was induced overnight at 22°C and cells were shifted to 32°C when required. Strain AB33ΔKin3_rDyn1_GRab5a was grown over night in complete medium (CM) containing 1% (w/v) arabinose. Hyphal growth was induced by shifting in NM liquid medium supplemented with 1% arabinose for 8 hours. For dynein depletion, cells were shifted to NM liquid medium supplemented with 1% glucose for 12 to 14 hours.

Laser-based epi-fluorescent microscopy

Microscopy was done essentially as previously described (Schuster et al, 2011a,b). In brief, hyphal cells were placed on a 2% agar cushion and cargo or motor motility was observed using an IX81 motorized inverted microscope (Olympus, Hamburg, Germany) equipped with a VS-LMS4 Laser-Merge-System using solid state lasers (488 nm/ 75mW and 561 nm/75 mW, Visitron System, Munich, Germany). Photo-activation and photo-bleaching experiments were done using a Visitron 2D FRAP system (Visitron System, Munich, Germany) consisting of a 405 nm/ 60 mW diode laser, which was dimmed by a ND 0.6 filter resulting in 15 mW output power. Simultaneous observation of red and green fluorescent protein fluorescence was done using a Dual-View Microimager (Optical Insights, Tucson, USA) and filter sets consisting of excitation dual line beam splitter (z491/561, Chroma, Rockinham, USA), the emission beam splitter in the DualView (565 DCXR, Chroma, Rockinham, USA), an ET-Bandpass 525/50 (Chroma, Rockinham, USA) and a BrightLine HC 617/73 (Samrock, Rochester, USA). For temperature-dependent experiments the objectives were cooled or heated using metal hull connected to a water bath (Huber, Offenburg, Germany). Images were captured using a Charged-Coupled Device camera (Photometric CoolSNAP HQ2, Roper Scientific, Germany). All parts of the microscope system were under the control of the software package MetaMorph (Molecular Devices, Downingtown, USA).

Analysis of microtubule bundling

Hyphal cells were fixed with 1% formaldehyde (Polyscience) to avoid MT motility. Z-stacks were taken at 300 nm step size using a Piezo drive (Piezosystem Jena GmbH, Jena, Germany). Z-stacks of MTs were processed

by 100 iterations of three-dimensional (3D) deconvolution. Maximum projections, cross-sections and 3D reconstructions of the resulting images were created using AutoQuantX software (AutoQuant Imaging, Troy, NYC). Fluorescence intensity measurements of the microtubule signals were carried out using MetaMorph. To determine the intensity of single MTs, the mean fluorescent intensity of the 10 faintest singles was determined. The degree of microtubule bundling was estimated by comparison to these signals.

Visualization and analysis of the run-length of fluorescent motor proteins and EEs

Motors were visualised in hyphal cells of strains AB33Kin3G, AB33G_3Dyn2 and AB33ΔKin3_Kin3^{ts}_G_3Dyn2. To visualize retrograde motility of motors 2 different sets of image series were acquired. The extended runs were investigated by photo-bleaching the whole cell (excluding the apical 10 µm) with a 405 nm laser at 100% output power at 150 ms exposure and beam diameter of 30 pixels using the UPlanSApo 60X/1.35 Oil objective. After a pause for 10 seconds, streams of 400 planes were taken using a 488 nm observation laser at 40% output power at an exposure time of 250 ms, a 250 ms interval between frames and image binning 2. For short runs a second set of image series was acquired using a PlanApo 100X/1.45 Oil TIRF objective. In this case only 30-40 µm of the hyphal cell was photo-bleached, but excluding the apical 3-5 µm. This was followed by immediate observation by using the 488 nm observation laser at 100% output power at 50 ms exposure time. For each strain the “long” and the “short” set was comprised of 20 movies and the run-length were analysed in kymographs that were generated from these image series using MetaMorph.

For analysis of the temperature-sensitive strains AB33ΔKin3_Kin3^{ts}_G_3Dyn2 and AB33ΔKin3_Kin3^{ts}_paGRab5a the objective and the agar pads were pre-cooled to 22°C or pre-heated to 32°C before the hyphal cells were observed. Inactivation of kinesin-3^{ts} was done by either pre-incubating the culture at 32°C for 5 min (for AB33ΔKin3_Kin3^{ts}_G_3Dyn2) or by keeping cells on the pre-warmed microscope stage for ~3 minutes before image series were taken. Dynein motility in AB33ΔKin3_Kin3^{ts}_G_3Dyn2 was recorded as described above, whereas EE motility in AB33ΔKin3_Kin3^{ts}_GRab5a was observed at 15% output power of the 488 nm laser at 150 ms exposure time and binning 1. Photo-activation of EEs in strains AB33paGRab5a and AB33ΔKin3_Kin3^{ts}_paGRab5a was done with a 100 ms light pulse using a 60 mW 405nm laser at 2% output power. Image series of 600 frames were taken with the 488 nm observation laser at 15% output power, an exposure time of 100 ms, image interval of 300 ms and image binning 2. Run-length were analysed in kymographs that were generated from these images using MetaMorph.

Analysis of the co-localisation of EE with Dynein and Kinesin-3

To analyse the degree of co-localisation of kinesin-3 and EE in strain AB33ΔKin3_Kin3G_ChRab5a, a region of 10 µm in length at 5 µm behind the tip or septum or around the nucleus was irradiated by using 100% output power of 405 nm laser for 75 ms with a beam diameter of 30 pixels. This was followed by immediate observation by using the Dual-View Microimager and the 488 nm observation laser at 100% output power and the 561nm observation laser at 25% output power at an exposure time of 200 ms and image binning 1. Kymographs from both fluorescent channels were overlaid and co-localization

was analysed. For the co-localisation of dynein and EEs 50 µm of the hyphal cell, beginning 5 µm behind the tip, was photo-bleached with the 405 nm laser at 100% output power for 150 ms with a beam diameter of 30 pixels. Subsequently, 100 frame movies were taken without delay or after 10 or 15 seconds using the 488 nm observation laser at 70% output power and the 561 laser at 30% output power and an exposure time of 150 ms. Again kymographs were merged and the degree of co-localisation was analysed in these overlaid images.

Supplementary data

Supplementary data are available at The EMBO Journal Online (http://www.embojournal.org).

Conflict of interest

The authors declare no conflict of interest.

Author Contributions

MS has performed experiments, generated strains and analyzed data; SK has generated the temperature-sensitive *kin3*^{ts} allele and Kin3^{ts} strains; GF has analyzed the degree of MT-bundling; JC generated strain AB33ΔKin3_Kin3G_ChRab5a and acquired and analyzed the co-localization data; YR generated strain AB33ΔKin3_rDyn1_GRab5a and analyzed the co-localization of EEs and dynein; GS has conceived the project, designed and analyzed data, written the manuscript, and provided overall project management.

REFERENCES

Abenza JF, Pantazopoulou A, Rodriguez JM, Galindo A, Penalva MA (2009) Long-distance movement of *Aspergillus nidulans* early endosomes on microtubule tracks. *Traffic (Copenhagen, Denmark)* **10:** 57-75

Adamikova L, Straube A, Schulz I, Steinberg G (2004) Calcium signaling is involved in dynein-dependent microtubule organization. *Mol Biol Cell* **15:** 1969-1980

Ally S, Larson AG, Barlan K, Rice SE, Gelfand VI (2009) Opposite-polarity motors activate one another to trigger cargo transport in live cells. *J Cell Biol* **187:** 1071-1082

Baas PW (1999) Microtubules and neuronal polarity: lessons from mitosis. *Neuron* **22:** 23-31

Baas PW, Deitch JS, Black MM, Banker GA (1988) Polarity orientation of microtubules in hippocampal neurons: uniformity in the axon and nonuniformity in the dendrite. *Proc Natl Acad Sci* **85:** 8335-8339

Baas PW, Lin S (2010) Hooks and comets: The story of microtubule polarity orientation in the neuron. *Dev Neurobiol. Epub.*

Baas PW, Slaughter T, Brown A, Black MM (1991) Microtubule dynamics in axons and dendrites. *J Neurosci Res* **30:** 134-153

Barkus RV, Klyachko O, Horiuchi D, Dickson BJ, Saxton WM (2008) Identification of an axonal kinesin-3 motor for fast anterograde vesicle transport that facilitates retrograde transport of neuropeptides. *Mol Biol Cell* **19:** 274-283

Black MM, Baas PW (1989) The basis of polarity in neurons. *Trends Neurosci.* **12:** 211-214

Bottin A, Kämper J, Kahmann R (1996) Isolation of a carbon source-regulated gene from *Ustilago maydis*. *Mol Gen Genet* **253:** 342-352

Brachmann A, Weinzierl G, Kämper J, Kahmann R (2001) Identification of genes in the bW/bE regulatory cascade in Ustilago maydis. *Mol Microbiol* **42:** 1047-1063

Burton PR, Paige JL (1981) Polarity of axoplasmic microtubules in the olfactory nerve of the frog. *Proc Natl Acad Sci* **78:** 3269-3273

Chevalier-Larsen E, Holzbaur EL (2006) Axonal transport and neurodegenerative disease. *Biochim Biophys Acta* **1762:** 1094-1108

Deacon SW, Nascimento A, Serpinskaya AS, Gelfand VI (2005) Regulation of bidirectional melanosome transport by organelle bound MAP kinase. *Curr Biol* **15:** 459-463

Deacon SW, Serpinskaya AS, Vaughan PS, Lopez Fanarraga M, Vernos I, Vaughan KT, Gelfand VI (2003) Dynactin is required for bidirectional organelle transport. *J Cell Biol* **160:** 297-301

Delcroix JD, Valletta JS, Wu C, Hunt SJ, Kowal AS, Mobley WC (2003) NGF signaling in sensory neurons: evidence that early endosomes carry NGF retrograde signals. *Neuron* **39:** 69-84

Duncan JE, Goldstein LS (2006) The genetics of axonal transport and axonal transport disorders. *PLoS Genetics* **2:** e124

Gross SP (2004) Hither and yon: a review of bi-directional microtubule-based transport. *Phys Biol* **1:** R1-11

Gross SP, Tuma MC, Deacon SW, Serpinskaya AS, Reilein AR, Gelfand VI (2002a) Interactions and regulation of molecular motors in *Xenopus* melanophores. *J Cell Biol* **156:** 855-865

Gross SP, Welte MA, Block SM, Wieschaus EF (2002b) Coordination of opposite-polarity microtubule motors. *J Cell Biol* **156:** 715-724

Guillaud L, Wong R, Hirokawa N (2008) Disruption of KIF17-Mint1 interaction by CaMKII-dependent phosphorylation: a molecular model of kinesin-cargo release. *Nat Cell Biol* **10:** 19-29

Ha J, Lo KW, Myers KR, Carr TM, Humsi MK, Rasoul BA, Segal RA, Pfister KK (2008) A neuron-specific cytoplasmic dynein isoform preferentially transports TrkB signaling endosomes. *J Cell Biol* **181:** 1027-1039

Heidemann SR, Landers JM, Hamborg MA (1981) Polarity orientation of axonal microtubules. *J Cell Biol* **91:** 661-665

Hendricks AG, Perlson E, Ross JL, Schroeder HW, 3rd, Tokito M, Holzbaur EL (2010) Motor coordination via a tug-of-war mechanism drives bidirectional vesicle transport. *Curr Biol*

Higuchi Y, Nakahama T, Shoji JY, Arioka M, Kitamoto K (2006) Visualization of the endocytic pathway in the filamentous fungus *Aspergillus oryzae* using an EGFP-fused plasma membrane protein. *Biochem Biophys Res Comm* **340:** 784-791

Hirokawa N, Sato-Yoshitake R, Yoshida T, Kawashima T (1990) Brain dynein (MAP1C) localizes on both anterogradely and retrogradely transported membranous organelles in vivo. *J Cell Biol* **111:** 1027-1037

Hirokawa N, Takemura R (2004) Molecular motors in neuronal development, intracellular transport and diseases. *Curr Opin Neurobiol* **14:** 564-573

Howard J, Hudspeth AJ, Vale RD (1989) Movement of microtubules by single kinesin molecules. *Nature* **342:** 154-158

Howard RJ (1981) Ultrastructural analysis of hyphal tip cell growth in fungi: Spitzenkörper, cytoskeleton and endomembranes after freeze-substitution. *J. Cell Sci.* **48:** 89-103.

Howard RJ, Aist JR (1979) Hyphal tip cell ultrastructure of the fungus Fusarium: improved preservation by freeze-substitution. *J. Ultrastruc. Res.* **66:** 224-234.

Howe CL, Mobley WC (2005) Long-distance retrograde neurotrophic signaling. *Curr Opin Neurobiol* **15:** 40-48

Kapitein LC, Schlager MA, Kuijpers M, Wulf PS, van Spronsen M, MacKintosh FC, Hoogenraad CC (2010) Mixed microtubules steer dynein-driven cargo transport into dendrites. *Curr Biol* **20:** 290-299

Klumpp S, Lipowsky R (2005) Cooperative cargo transport by several molecular motors. *Proc Natl Acad Sci USA* **102:** 17284-17289

Koonce MP, Schliwa M (1986) Reactivation of organelle movements along the cytoskeletal framework of a giant freshwater ameba. *J Cell Biol* **103:** 605-612

Koushika SP, Schaefer AM, Vincent R, Willis JH, Bowerman B, Nonet ML (2004) Mutations in Caenorhabditis elegans cytoplasmic dynein components reveal specificity of neuronal retrograde cargo. *J Neurosci* **24:** 3907-3916

Larsen KS, Xu J, Cermelli S, Shu Z, Gross SP (2008) BicaudalD actively regulates microtubule motor activity in lipid droplet transport. *PloS One* **3:** e3763

Lee JR, Shin H, Ko J, Choi J, Lee H, Kim E (2003) Characterization of the movement of the kinesin motor KIF1A in living cultured neurons. *J Biol Chem* **278:** 2624-2629

Lenz JH, Schuchardt I, Straube A, Steinberg G (2006) A dynein loading zone for retrograde endosome motility at microtubule plus-ends. *EMBO J* **25:** 2275-2286

Ligon LA, Tokito M, Finklestein JM, Grossman FE, Holzbaur EL (2004) A direct interaction between cytoplasmic dynein and kinesin I may coordinate motor activity. *J. Biol Chem* **279:** 19201-19208

Mallik R, Petrov D, Lex SA, King SJ, Gross SP (2005) Building complexity: an in vitro study of cytoplasmic dynein with in vivo implications. *Curr Biol* **15:** 2075-2085

Miaczynska M, Pelkmans L, Zerial M (2004) Not just a sink: endosomes in control of signal transduction. *Curr Opin Cell Biol* **16:** 400-406

Miller KE, DeProto J, Kaufmann N, Patel BN, Duckworth A, Van Vactor D (2005) Direct observation demonstrates that Liprin-alpha is required for trafficking of synaptic vesicles. *Curr Biol* **15:** 684-689

Müller MJ, Klumpp S, Lipowsky R (2008) Tug-of-war as a cooperative mechanism for bidirectional cargo transport by molecular motors. *Proc Natl Acad Sci USA* **105:** 4609-4614

Nogales E, Whittaker M, Milligan RA, Downing KH (1999) High-resolution model of the microtubule. *Cell* **96:** 79-88

Pedersen LB, Geimer S, Rosenbaum JL (2006) Dissecting the molecular mechanisms of intraflagellar transport in chlamydomonas. *Curr Biol* **16:** 450-459

Pilling AD, Horiuchi D, Lively CM, Saxton WM (2006) Kinesin-1 and Dynein are the primary motors for fast transport of mitochondria in *Drosophila* motor axons. *Mol Biol Cell* **17:** 2057-2068

Reck-Peterson SL, Yildiz A, Carter AP, Gennerich A, Zhang N, Vale RD (2006) Single-molecule analysis of dynein processivity and stepping behavior. *Cell* **126:** 335-348

Rogers SL, Tint IS, Fanapour PC, Gelfand VI (1997) Regulated bidirectional motility of melanophore pigment granules along microtubules in vitro. *Proc Natl Acad Sci* **94:** 3720-3725

Schuchardt I, Assmann D, Thines E, Schuberth C, Steinberg G (2005) Myosin-V, Kinesin-1, and Kinesin-3 cooperate in hyphal growth of the fungus *Ustilago maydis*. *Mol Biol Cell* **16:** 5191-5201

Schulz B, Banuett F, Dahl M, Schlesinger R, Schafer W, Martin T, Herskowitz I, Kahmann R (1990) The b alleles of U. maydis, whose combinations program pathogenic development, code for polypeptides containing a homeodomain-related motif. *Cell* **60:** 295-306

Schuster M, Assmann MA, Lenz P, Lipowsky R, Steinberg G (2011a) Transient binding of dynein controls bidirectional long-range motility of early endosomes *Proc Natl Acad Sci USA* Epub ahead of print.

Schuster M, Kilaru S, Ashwin P, Congping L, Severs NJ, Steinberg G (2011b) Controlled and stochastic retention concentrates dynein at microtubule ends to keep endosomes on track. *EMBO J* Epub ahead of print.

Shubeita GT, Tran SL, Xu J, Vershinin M, Cermelli S, Cotton SL, Welte MA, Gross SP (2008) Consequences of motor copy number on the intracellular transport of kinesin-1-driven lipid droplets. *Cell* **135:** 1098-1107

Smith GA, Pomeranz L, Gross SP, Enquist LW (2004) Local modulation of plus-end transport targets herpesvirus entry and egress in sensory axons. *Proc Natl Acad Sci* **101:** 16034-16039

Soppina V, Rai AK, Ramaiya AJ, Barak P, Mallik R (2009) Tug-of-war between dissimilar teams of microtubule motors regulates transport and fission of endosomes. *Proc Natl Acad Sci USA* **106:** 19381-19386

Spee JH, de Vos WM, Kuipers OP (1993) Efficient random mutagenesis method with adjustable mutation frequency by use of PCR and dITP. *Nucleic Acids Res* **21:** 777-778

Steinberg G (2007) On the move: endosomes in fungal growth and pathogenicity. *Nat Rev Microbiol* **5:** 309-316

Steinberg G, Perez-Martin J (2008) *Ustilago maydis*, a new fungal model system for cell biology. *Trends Cell Biol* **18:** 61-67

Steinberg G, Schliwa M, Lehmler C, Bolker M, Kahmann R, McIntosh JR (1998) Kinesin from the plant pathogenic fungus Ustilago maydis is involved in vacuole formation and cytoplasmic migration. *J Cell Sci* **111 (Pt 15):** 2235-2246

Steinberg G, Schuster M (2011) The dynamic fungal cell. *Fungal Biol Rev* ***in press***

Steinberg G, Wedlich-Söldner R, Brill M, Schulz I (2001) Microtubules in the fungal pathogen *Ustilago maydis* are highly dynamic and determine cell polarity. *J Cell Sci* **114:** 609-622

Straube A, Brill M, Oakley BR, Horio T, Steinberg G (2003) Microtubule organization requires cell cycle-dependent nucleation at dispersed cytoplasmic sites: polar and perinuclear microtubule organizing centers in the plant pathogen Ustilago maydis. *Mol Biol Cell* **14:** 642-657

Straube A, Hause G, Fink G, Steinberg G (2006) Conventional kinesin mediates microtubule-microtubule interactions *in vivo*. *Mol Biol Cell* **17:** 907-916

Thorn KS, Ubersax JA, Vale RD (2000) Engineering the processive run length of the kinesin motor. *J Cell Biol* **151:** 1093-1100

Vale RD (2003) The molecular motor toolbox for intracellular transport. *Cell* **112:** 467-480

Wang Z, Khan S, Sheetz MP (1995) Single cytoplasmic dynein molecule movements: characterization and comparison with kinesin. *Biophys J* **69:** 2011-2023

Wedlich-Söldner R, Bölker M, Kahmann R, Steinberg G (2000) A putative endosomal t-SNARE links exo- and endocytosis in the phytopathogenic fungus *Ustilago maydis*. *EMBO J* **19:** 1974-1986

Wedlich-Söldner R, Straube A, Friedrich MW, Steinberg G (2002a) A balance of KIF1A-like kinesin and dynein organizes early endosomes in the fungus *Ustilago maydis*. *EMBO J* **21:** 2946-2957

Wedlich-Söldner R, Schulz I, Straube A, Steinberg G (2002b) Dynein supports motility of endoplasmic reticulum in the fungus *Ustilago maydis*. *Mol Biol Cell* **13:** 965-977

Welte MA (2004) Bidirectional transport along microtubules. *Curr Biol* **14:** R525-537

Welte MA, Cermelli S, Griner J, Viera A, Guo Y, Kim DH, Gindhart JG, Gross SP (2005) Regulation of lipid-droplet transport by the perilipin homolog LSD2. *Curr Biol* **15:** 1266-1275

Welte MA, Gross SP, Postner M, Block SM, Wieschaus EF (1998) Developmental regulation of vesicle transport in *Drosophila* embryos: forces and kinetics. *Cell* **92:** 547-557

Zheng Y, Wildonger J, Ye B, Zhang Y, Kita A, Younger SH, Zimmerman S, Jan LY, Jan YN (2008) Dynein is required for polarized dendritic transport and uniform microtubule orientation in axons. *Nature cell biology* **10:** 1172-1180

Zhou HM, Brust-Mascher I, Scholey JM (2001) Direct visualization of the movement of the monomeric axonal transport motor UNC-104 along neuronal processes in living *Caenorhabditis elegans*. *J Neurosci* **21:** 3749-3755

Figures and legends

Figure 1
Schuster et al.

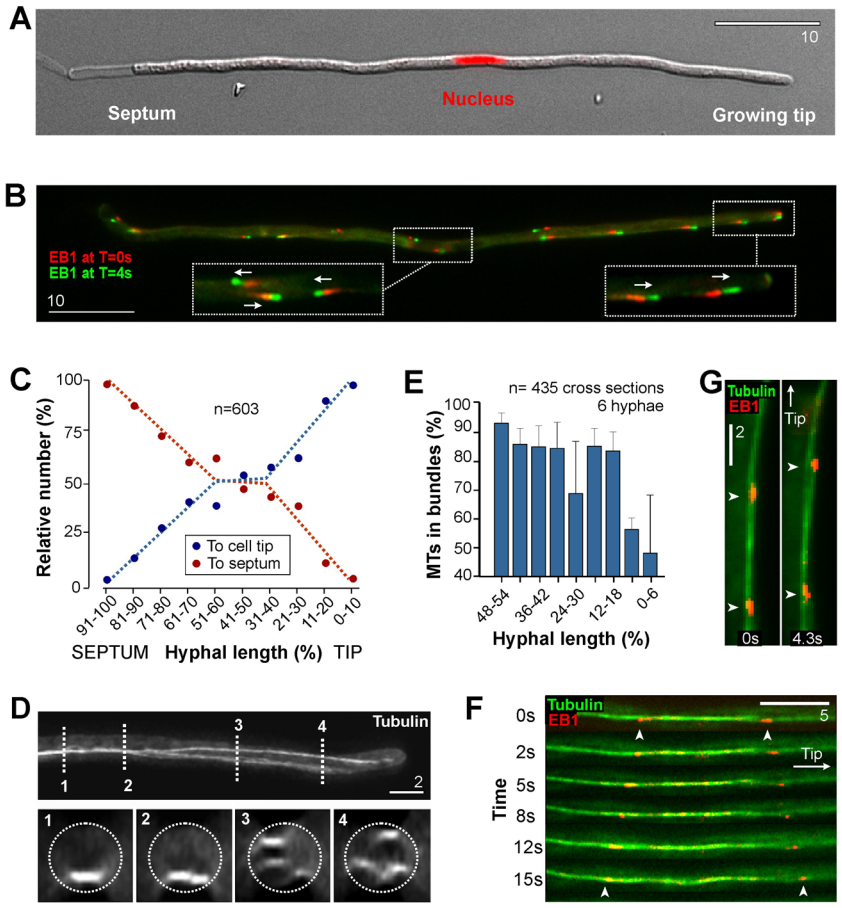

Figure 1 Microtubule organization in hyphal cells of *Ustilago maydis*

(**A**) Hyphal cell of *Ustilago maydis.* The elongated cell extends at the tip and forms a septum at the rear cell pole. The nucleus is positioned near the cell center. Bar represents micrometers.

(**B**) Overlay of two images showing Peb1-YFP motility in a hyphal cell. Bar represents micrometers. See supplementary Movie S1.

(**C**) Graph indicating the orientation of Peb1-YFP motility in hyphal cells. Peb1 is a homologue of EB1 and labeled growing MT plus-ends. At the cell poles MTs are mainly uni-polar, whereas the array is bi-polar in most central parts of the hypha.

(**D**) Maximum projection of a Z-axis stack of GFP-Tub1 labelled MTs in *U. maydis.* Near the hyphal tip ~50% of all MTs are gathered in brighter MT bundles (cross section 3 and 4). The degree of bundling increases towards the middle region of the cell (cross section 1 and 2). See supplementary Movie S2.

(**E**) Degree of bundling estimated from quantitative fluorescence microscopy on GFP-α-tubulin MTs. This method was previously validated by electron microscopy studies (Straube et al, 2006).

(**F**) Peb1-RFP-labeled plus-ends within a bi-polar MT bundle. The motility of the EB1-homologue indicates that the bundle consist of anti-polar oriented MTs. Time is indicated in seconds. Bar represents micrometer.

(**G**) Peb1-RFP-labeled plus-ends within a MT bundle. The motility of the EB1-homologue indicates that the bundle consist of uni-polar oriented MTs. Time is indicated in seconds. Bar represents micrometer.

Figure 2
Schuster et al.

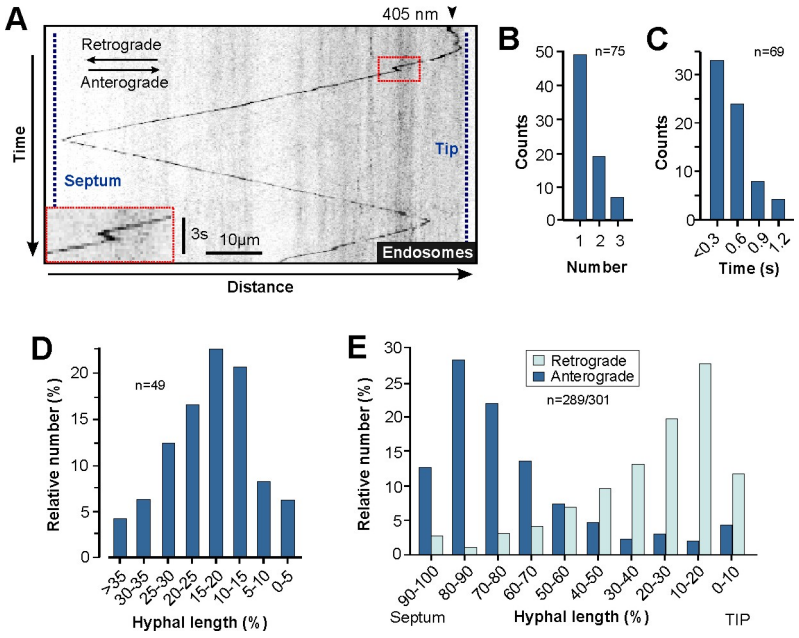

Figure 2 Motility of early endosomes labeled with photo-activatable paGFP-Rab5a.

(**A**) Kymograph showing motility of a paGFP-Rab5a carrying EE visualized after photo-activation with a 405 nm laser pulse at the hyphal tip (405nm). The organelle travels continuously to the rear end of the cell where it turns direction and travels back towards the hyphal tip. The inset shows a short inconsistency in the trajectory of the retrograde moving organelle. The bars represent micrometers and seconds. See supplementary Movie S3.

(**B**) Bar chart showing the number of pauses in retrograde EE trajectories. Sample size *n* is given. Measurements were done using photo-activated paGFP-Rab5a-carrying EEs.

(**C**) Bar chart showing the pausing time per irregularity of retrograde EE runs. Sample size *n* is given. Measurements were done using photo-activated paGFP-Rab5a-carrying EEs.

(**D**) Bar chart showing the position of the first irregularity in the retrograde trajectory. Sample size *n* is given. Measurements were done using photo-activated paGFP-Rab5a-carrying EEs.

(**E**) Run-length of EEs photo-activated at the hyphal tip (light blue) or at the septum (dark blue) of hyphal cells. Sample size *n* is given.

Figure 3
Schuster

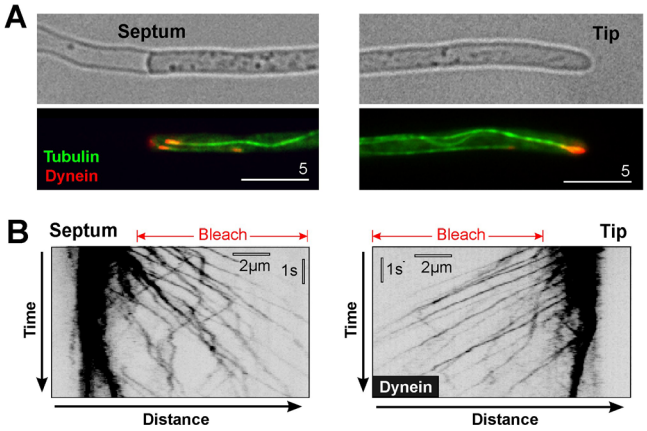

Figure 3 Dynein accumulations at MT ends near the tip and the septum.

(**A**) GFP_3-Dynein forms comets at MT ends (GFP-Tub1) near the septum and the growing tip. Note that dynein comets are regions of efficient EE capturing and are therefore considered a "loading zone" where arriving EEs bind to dynein for retrograde transport (Lenz et al, 2006; Schuster et al, 2011b). Bar represents micrometers.

(**B**) Kymographs showing GFP_3-dynein leaving the dynein comets near the septum and the hyphal tip. Cells were photo-bleached to reduce the interfering signal background. Images were contrast inverted. Bars represent micrometers and seconds.

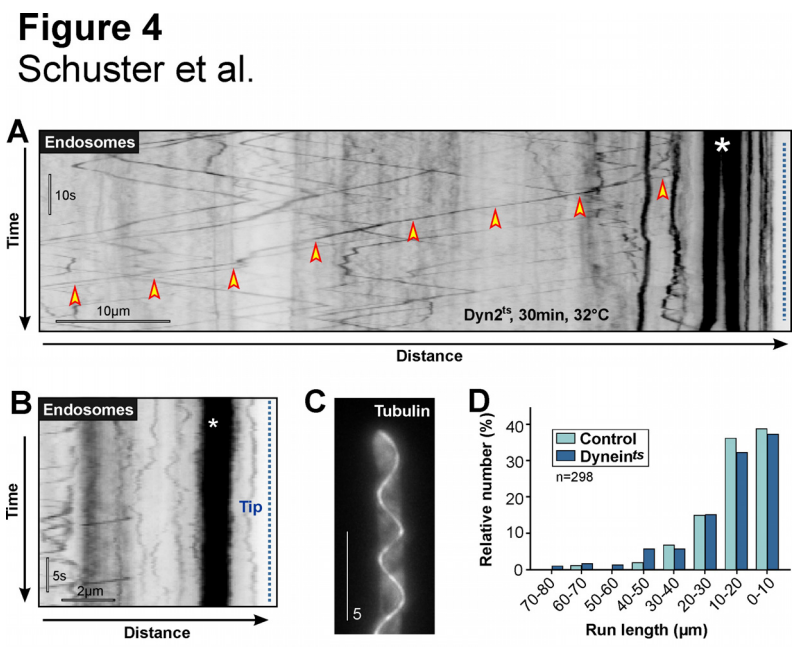

Figure 4 Retrograde motility of EEs in conditional dynein mutants.

(**A**) Kymograph showing retrograde motility EEs (GFP-Rab5a) in a Dyn2^{ts} mutant hypha. EEs still show long-range motility. The cell was shifted to 32°C for 30 minutes. Bars represent micrometers and seconds. For control kymograph at 22°C see supplementary Figure S1; see supplementary Movie S4.

(**B**) Kymograph showing EEs (GFP-Rab5a) in the apical region of a temperature-sensitive *dyn2*^{ts} hyphal cell. EEs cluster at plus-ends near the hyphal cell tip (asterisk). No motility is seen, indicating that dynein is inactivated. Note that MTs in this region have a uni-polar orientation. The cell was shifted to 32°C for 30 minutes. Bars represent micrometers and seconds.

(**C**) Images showing MTs (GFP-Tub1) in a Dyn2^{ts} mutant hypha at restrictive temperature. In the absence of dynein MTs become longer and often reach into the apex of the hyphal cell. The effect of dynein inactivation on MT length was reported previously (Adamikova et al, 2004). Bar represent micrometer.

(**D**) Bar chart showing retrograde run-length of EEs in a *dyn2*^{ts} mutant cell at restrictive temperature. Note that no motility was seen in the first 10 µm in *dyn2*^{ts} mutants. To compare this sub-apical motility with control cells at restrictive temperature, the run-length of EEs in control cells was measured starting 10 µm behind the tip.

Figure 5
Schuster et al.

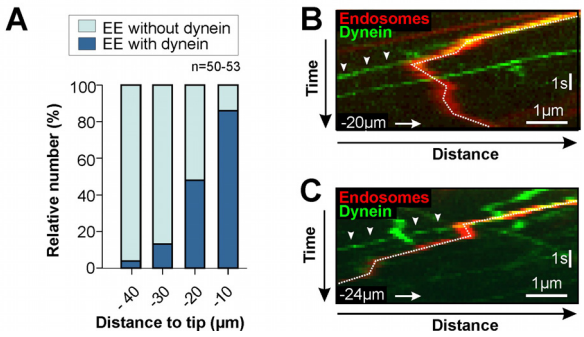

Figure 5 Co-localization of GFP_3-dynein and mCherry-Rab5a on retrograde EEs.

(**A**) Bar chart showing the degree of co-localization of dynein and EEs. At each position 50-53 retrograde-moving organelles were analyzed.

(**B**) Kymograph showing motility of mCherry-Rab5a on EEs (red) and motility of GFP_3-dynein heavy chain (green). Dynein and the EE travel together until the EE turns direction, whereas dynein continuous motility. The position relative to the tip is shown in the lower left corner, the location of the cell tip is indicated (arrow and "Tip"). The path of the EE is indicated by a dotted line. The bars represent micrometers and seconds.

(**C**) Kymograph showing motility of mCherry-Rab5a on EEs (red) and motility of GFP_3-dynein heavy chain (green). Dynein and the EE travel together until the EE pauses for ~1 second, whereas dynein continuous motility. After the pause the EE continuous retrograde motility independent of dynein. The position relative to the tip is shown in the lower left corner, the location of the cell tip is indicated (arrow and "Tip"). The path of the EE is indicated by a dotted line. The bars represent micrometers and seconds.

Figure 6
Schuster et al.

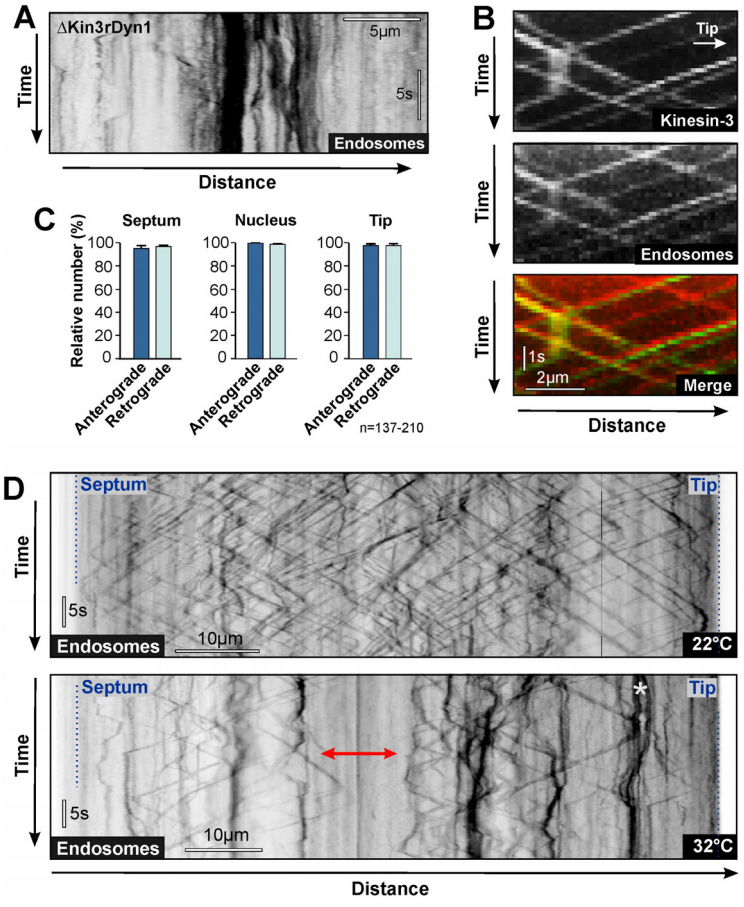

Figure 6 Run-length of EEs in temperature-sensitive kinesin-3 mutants.

(**A**) Kymograph showing EE (GFP-Rab5a) motility in hyphal cells of a conditional dynein/Δkinesin-3 double mutant. Motility is abolished (indicate by vertical lines). Bars represent micrometers and seconds. See supplementary Movie S6.

(**B**) Kymographs showing co-migration of kinesin-3-GFP and EEs (labeled with mCherry-Rab5a). Kinesin-3 is bound to anterograde and retrograde organelles. Bars represent micrometers and seconds.

(**C**) Bar chart showing the relative number of kinesin-3-GFP co-localized with mCherry-Rab5a labeled EE. Note that only few kinesin-3 motors do not co-localize with EEs. Anterograde: motility towards the hyphal tip; retrograde: motility towards the septum.

(**D**) Kymographs showing motility of EEs in a Kin3^{ts} mutant at permissive (22ºC) and restrictive (32 ºC) temperature. Note that at restrictive temperature EE clusters are formed (asterisk) and EEs motility did not overcome the middle part of the cell (red arrow), thereby no longer connecting the apical and the rear cell regions. Cell ends are indicated by dotted lines and “Septum” and “Tip”. Bars represent micrometers and seconds.

Figure 7
Schuster et al.

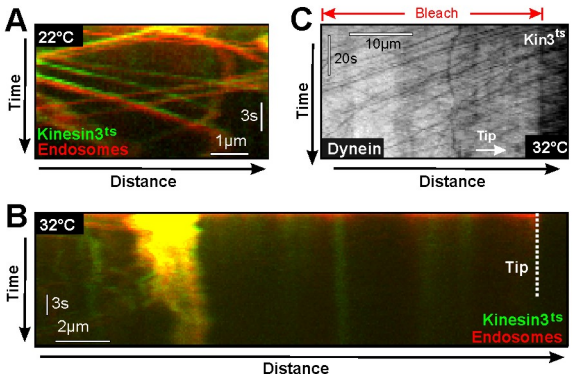

Figure 7 Motility of EEs, dynein and the temperature-sensitive kinesin-3^{ts} protein in kinesin-3 mutants.

(**A**) Kymograph showing co-localization of the temperature-sensitive mutant motor protein Kinesin-3^{ts}-GFP and mCherry-Rab5a at permissive temperature. The motor localizes to anterograde and retrograde EEs. Bars represent micrometers and seconds.

(**B**) Kymograph showing co-localization of the temperature-sensitive mutant motor protein kinesin-3^{ts}-GFP and mCherry-Rab5a after 5 minutes at restrictive temperature. Kinesin-3^{ts}-GFP still localizes to the EEs, which have left the apical region of the hyphal cell and form large aggregates at ~10 µm behind the cell tip. The position of the hyphal tip is indicated (Tip). See supplementary Movie S8.

(**C**) Kymograph showing retrograde motility of GFP-labeled dynein in kinesin-3^{ts} cells at restrictive temperature. Cells were pre-bleached (indicated by red arrow and “bleach”) using a 405 nm to reduce the interference with anterograde moving dynein signals (Schuster et al, 2011a, b).

Figure 8
Schuster et al.

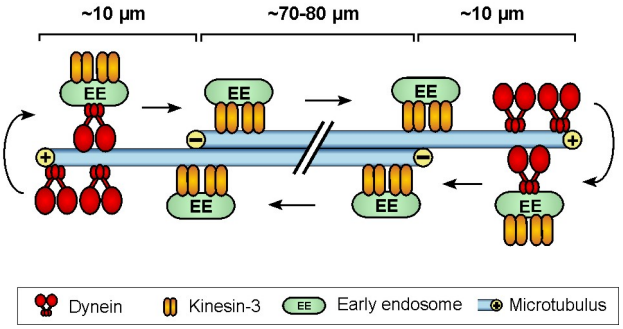

Figure 8 Model for motor cooperation in long-range retrograde EE motility.

EEs arrive at MT plus-ends and get loaded onto dynein that takes the organelles through the uni-polar MT array towards minus-ends. At this time kinesin-3 is a passive cargo. At ~10 µm behind the tip anti-polar bundles allow kinesin-3 to take over and kinesin-3 motors transport the EEs towards plus-ends at the rear cell pole

Table 1. Strains and plasmids used in this study

AB33nRFP	*a2* P*narbW2* P*narbE1, ble*^{R} / poNLS3RFP	Schuster et al, 2011a
AB33EB1Y	*a2* P*narbW2* P*narbE1*, P*peb1-peb1-yfp*, *ble*^{R}, *nat*^{R}	This study
AB33GT	*a2* P*narbW2* P*narbE1, ble*^{R} / potefGFPTub1	This study
AB33GT_Peb1R	*a2* P*narbW2* P*narbE1,* P*peb1-peb1-rfp*, *ble*^{R}, *nat*^{R} / potefGFPTub1	Schuchhardt et al, 2005
AB33paGRab5a	*a2* P*narbW2* P*narbE1, ble*^{R} / popaGRab5a	Schuster et al, 2011a
AB33Ch$_3$Dyn2_GT	*a2* P*narbW2* P*narbE1*, P*dyn2-3xmCherry-dyn2, ble*^{R}, *hyg*^{R} / potefGFPTub1	This study
AB33G$_3$Dyn2	*a2* P*narbW2* P*narbE1*, P*dyn2-3xegfp-dyn2, ble*^{R}, *hyg*^{R}	Lenz et al., 2006
AB33G$_3$Dyn2_ChRab5a	*a2* P*narbW2* P*narbE1*, P*dyn2-3xegfp-dyn2*, *ble*^{R}, *hyg*^{R} / po$_m$ChRab5a	Schuster et al, 2011a
AB5Dyn2^{ts}_GRab5a	*a1*P*narbW2* P*narbE1*, P*dyn2-dyn2^{ts}*, *ble*^{R}, *hyg*^{R} / poGRab5a	This study
AB5Dyn2^{ts}_GT	*a1*P*narbW2* P*narbE1*, P*dyn2-dyn2^{ts}*, *ble*^{R}, *hyg*^{R} / potefGFPTub1	This study
AB33Kin3G	*a2* P*narbW2* P*narbE1*, P*kin3-kin3-egfp, ble*^{R}, *hyg*^{R}	This study
AB33ΔKin3_Rab5a	*a2* P*narbW2* P*narbE1,* Δ*kin3, ble*^{R}, *nat*^{R} / poGRab5a	This study
AB33ΔKin3_rDyn1_GRab5a	*a2* P*narbW2* P*narbE1,* Δ*kin3, Pcrg-dyn1, ble*^{R}, *nat*^{R}, *hyg* ^{R} / poGRab5a	This study
AB33ΔKin3_Kin3G_ChRab5a	*a2* P*narbW2* P*narbE1,* Δ*kin3, ble*^{R}, *hyg*^{R} / pKin3G / po$_m$ChRab5a	This study
AB33ΔKin3_Kin3^{ts}_GRab5a	*a2* P*narbW2* P*narbE1,* Δ*kin3, ble*^{R}, *nat*^{R}, / pKin3^{ts} / poGRab5a	This study
AB33ΔKin3_Kin3^{ts}_paGRab5a	*a2* P*narbW2* P*narbE1,* Δ*kin3, ble*^{R}, *nat*^{R}, / pKin3^{ts} / popaGRab5a	This study
AB33ΔKin3_Kin3^{ts}G_tagRRab5a	*a2* P*narbW2* P*narbE1,* Δ*kin3, ble*^{R}, *nat*^{R},/ pKin3^{ts}G / potagRRab5a	This study
AB33ΔKin3_G$_3$Dyn2_Kin3^{ts}	*a2* P*narbW2* P*narbE1,* Δ*kin3,* P*dyn2-3xegfp-dyn2, ble*^{R}, *nat*^{R}, *cbx*^{R} / pKin3^{ts}	This study
poNLS3RFP	P*otef-gal4$_s$-mrfp-mrfp-mrfp, nat*^{R}	Schuster et al, 2011a
potefGFPTub1	P*otef-egfp-tub1, cbx*^{R}	Steinberg et al, 2001
popaGRab5a	P*otef-pagfp-rab5a, cbx*^{R}	Schuster et al, 2011b
po$_m$ChRab5a	P*otef-mcherry-rab5a, nat*^{R}	Schuster et al, 2011a
poGRab5a	P*otef-egfp-rab5a, nat*^{R}	Schuster et al, 2011b
pKin3G	P*kin3-kin3-gfp, cbx*^{R}	Wedlich-Söldner, et al, 2002a
pKin3^{ts}	P*kin3-kin3^{ts}, hyg*^{R}	This study
pKin3^{ts}G	P*kin3-kin3^{ts}-gfp, hyg*^{R}	This study
potagRRab5a	P*otef-tagrfp-rab5a, cbx*^{R}	This study

a, *b*, mating type loci; P, promoter; -, fusion; *hyg*^{R}, hygromycin resistance; *ble*^{R}, phleomycin resistance; *nat*^{R}, nourseothricin resistance; *cbx*^{R}, carboxin resistance; ^{ts}, temperature-sensitive allele; Δ, deletion; /, ectopically integrated; *crg*, conditional arabinose-induced promoter; *otef*, constitutive promoter; *nar*, conditional nitrate reductase promoter; *E1*, *W2*, genes of the *b* mating type locus; *egfp*, enhanced green fluorescent protein; *pagfp:* photoactivatable monomeric green fluorescent protein; *mrfp* and *tagrfp* , monomeric red fluorescent protein; *mcherry*, monomeric cherry; *yfp*, yellow fluorescent protein; NLS, nuclear localization signal of the GAL-4 DNA binding domain from pC-ACT1 (Clontech); GT, gfp-tubulin; *peb1*, EB1-like plus-end binding protein; *dyn2*: C-terminal half of the dynein heavy chain; *dyn1*: N-terminal half of the dynein heavy chain *rab5a*, small endosomal Rab5-like GTPase; *kin3*, kinesin-3;

Supplementary Information

Figure S1
Schuster et al.

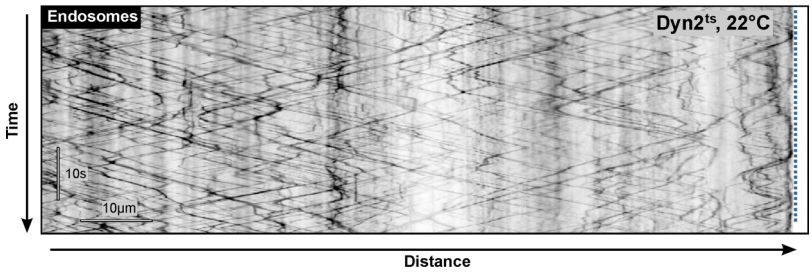

Figure S1 Bi-directional of EEs in temperature-sensitive dynein mutants at permissive temperature. Bar represents micrometers; time is given in seconds and milliseconds.

Figure S2
Schuster et al.

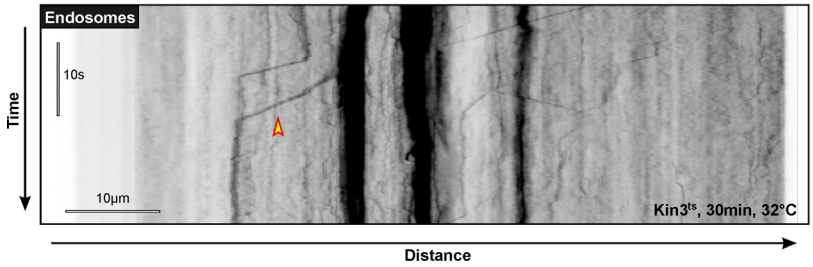

Figure S2 Distribution of EEs in kinesin-3^{ts} mutants after 30 minutes at restrictive conditions. Clusters of GFPRab5a-labeled EEs are now found predominantly in the middle part of the hyphal cell and very little motility occurs (arrowhead). Note that the phenotype of the cells varied and that some cells showed more motility. Bar represents micrometers; time is given in seconds and milliseconds.

Supplementary Movie legends

Movie S1 Motility of the EB1-homolouge Peb1-YFP in a hyphal cell. Peb1-YFP motility indicates growth of MT plus-ends. Bar represents micrometers; time is given in seconds and milliseconds.

Movie S2 MT organization in the hyphal cell. Sections are 3D-reconstructions of deconvolved Z-stacks. Note that cells were mildly fixed to avoid MT motility. Bar represents micrometers.

Movie S3 Retrograde motility of EEs after photo-activation of paGFP-Rab5a. The position of laser activation is indicated by blue arrowhead in first frame. The organelle migrates towards the septum at the rear cell end. Note the short pause near the hyphal tip (yellow arrowhead). Bar represents micrometers; time is given in seconds and milliseconds.

Movie S4 Motility of EEs in temperature-sensitive dynein mutants.

At restrictive temperature (32°C for 30 minutes), EEs accumulate near the hyphal apex, which is due to the unbalanced activity of kinesin-3 (Lenz et al, 2006). Retrograde motility within the apical region is abolished, whereas long-range motility is found in sub-apical regions. Note that MTs are uni-polar in the apical region with minus-ends being directed towards the cell center. Bar represents micrometers; time is given in seconds and milliseconds.

Movie S5 Dynein and retrograde EE trafficking.

EEs (red, labeled by mCherry-Rab5a) travel into a photo-bleached area. Dynein signals (green, labeled by GFP_3-Dyn2) travel independent of EEs (indicated by

"1") or co-localize with retrograde EEs (indicated by "2"). In addition, retrograde EEs move without co-localizing (indicated by "3"). Note that the microscopic setup allows visualization of individual dynein motors (Schuster et al, 2011a; Schuster et al, 2011b), suggesting that these retrograde EEs move independently of dynein. The distance to the hyphal tip to the right is indicated (arrowhead, -20 µm). Bar represents micrometers; time is given in seconds and milliseconds.

Movie S6 EEs in a conditional dynein-Δkinesin-3 double mutant.

Cells were grown in glucose-containing medium, which down regulates the *crg*-promoter, under which the dynein heavy chain gene *dyn1* was expressed. Depletion of dynein in the kinesin-3 null mutant abolished all EE motility. This strongly suggests that dynein and kinesin-3 are the only motors involved in EE motility. Cells were grown into hyphae in arabinose-containing medium and shifted to restrictive glucose-containing medium for 12-14 hours. Bar represents micrometers; time is given in seconds and milliseconds.

Movie S7 Retrograde motility of kinesin-3.

To reduce signal interference, all sub-apical parts of a hyphal cell of strain AB33Kin3G were photo-bleached by a 405nm laser. Kinesin-3 could be a passive cargo on retrograde EEs. However, the orientation of MTs allows and active role of kinesin-3 in transports towards the septum. Bar represents micrometers; time is given in seconds and milliseconds.

Movie S8 Motility of temperature-sensitive Kin3^{ts} and EEs at restrictive temperature.

In the temperature-sensitive mutant strain AB33ΔKin3_Kin3^{ts}G_tagRRab5a, the EEs form a cluster behind the hyphal tip. The mutant motor protein kinesin-3^{ts} still binds to these organelles. The apical region, where MTs have a uni-polar orientation, is devoid of organelles, which is due to the activity of dynein. In sub-apical areas MTs have a bi-polar orientation. Dynein is able to support short-range motility (see left of the EE cluster). Cells were shifted to 32°C for 5-10 minutes. Bar represents micrometers; the time is given in seconds and milliseconds.

5. General conclusion

5.1 The Microtubules in the hyphal cell of *U. maydis* are symmetrically organized

Transport of organelles in a bi-directional fashion is a remarkable attribute of eukaryotic cells (Gross, 2004; Welte, 2004). The molecular basis, by which the involved molecular motors work together, to move their cargos, is under intensive examination. In this work, I used the basidiomycete fungus *Ustilago maydis* to get a better understanding of this process. In *U. maydis,* early endosomes move bi-directionally along microtubules (Lenz et al., 2006; Wedlich-Söldner et al., 2000; Wedlich-Söldner et al., 2002a). Interestingly, in hyphal cells of this fungus, the microtubules form a non-uniform bi-polar microtubule array. In the centre of the cell, anti-polar bundles are concentrated, whereas the microtubules form uni-polar arrays at the cell poles with the plus ends being oriented outwards. The symmetry of this microtubule array is reflected by the motility behaviour of the early endosomes and the way the dynein transport machinery is organised. Dynein accumulates at the ends of the microtubule array at both cell poles. From here, it is released towards the cell centre and when meeting a kinesin-3-delivered early endosome dynein turns its transport direction. As a consequence, the run length of the organelles towards the cell centre follows the same distribution in both halves of the cell. Thus, the symmetric organisation of the microtubule array results in a balanced and symmetric behaviour of the organelles.

5.2. Dynein prevents early endosomes from falling off the microtubule

In fungi, the minus end directed motor dynein accumulates at the plus ends of microtubules (Lee et al., 2003; Sheeman et al., 2003; Xiang, 2003; Zhang et al., 2003; Lee et al., 2005; Lenz et al., 2006; Abenza et al., 2009; Zhang et al., 2010). In a previous study it was suggested that dynein gets delivered to the microtubule plus ends in an inactive state by kinesin-1 (Lenz et al., 2006). Here, it is thought to stay inactive until it binds to kinesin-3 delivered early endosomes. This step is thought to activate the motor and might trigger retrograde motility (Lenz et al., 2006). In the light of the data summarised in this thesis, this concept need to be revised. The key argument against the previously suggested concept comes from the fact that dynein is able to leave the microtubule plus ends without getting in contact with early endosomes. This clearly argues against a role of the organelles in activating dynein. Instead, dynein appears to bind to the anterograde organelles along the whole cell length and in a stochastic way. The random loading of organelles onto retrograde travelling dynein turns the organelles around, which is followed by transport towards the cell centre. However, if loading is a stochastic process, then there is a possibility that early endosomes arrive at microtubule plus ends without having met a dynein motor. At this point, the organelles might fall off the track and therefore the bidirectional transport process would be interrupted. The cell seems to avoid this scenario by increasing the number of dynein motors at microtubule plus-ends. The results summarised in the thesis suggest that it does this by a stochastic mechanism and active retention. The first mechanism assumes that dynein at the hyphal tip behaves similar to dynein travelling along the microtubule. In other words, no active turning or capturing mechanism influences the behaviour of dynein. Under these assumptions, about half of the

dynein motors in the apical comets can be explained. Indeed, the observation of dynein dynamics at microtubule plus ends supports the notion that two populations of dynein motors exist in the comet. A highly dynamic population, which has a turn-over half-life time of around 10s, whereas a second population stays much longer within the comet. The other mechanism by which the cell increases the dynein number at plus ends (and thereby the chances to capture an endosome) is by actively binding dynein to the microtubule tips. In epithelial cells and fibroblasts, dynactin interact with the plus-end binding protein EB1 (Ligon et al., 2003; Honnappa et al., 2006) and forms comet-like structures at the microtubule plus ends. A recent study also showed that dynein accumulates at the plus ends in mammalian cells (Kobayashi and Murayama, 2009). This suggested that anchorage of dynein in *U. maydis* might be mediated by an interaction of dynactin and the EB1 homologue Peb1 (Straube et al., 2003). Indeed, the expression of peptides that mimicked the Dya1 and Peb1 interaction site reduced the number of the dynein motors in the comet by 50-60%. This suggests that active retention of dynein via anchorage to the plus end-binding Peb1 helps to increase the motor number in the comet. When the Peb1-based retention mechanism is inhibited, kinesin-3-delivered early endosomes tend to fall off at the end of the microtubule. Taken together, this indicates that the loading process of endosomes onto dynein is stochastic and that the cell increases the chances of dynein interacting with early endosomes by increasing the number of motors in the comet.

5.3 A single dynein overcomes three to five kinesin-3 motors

Kinesin-3 and dynein cooperate in the bi-directional motility of early endosomes. The stochastic loading of the organelles onto dynein can occur along the length

of the hyphal cell and binding of dynein always turned the transport direction from anterograde to retrograde. To get a better understanding how dynein and kinesin-3 cooperation in this process, I analysed the numbers of those motor proteins. Using two independent methods, I could demonstrate that a single dynein wins over three to five kinesin-3 motors. It was shown in other cell systems that few motors are bound to the organelles, and the numbers measured on early endosomes matched these reports (Shubeita et al., 2008; Soppina et al., 2009; Hendricks et al., 2010). However, endosomal vesicles in primary neurons (Hendricks et al., 2010) and lipid droplets in flies (Shubeita et al., 2008) are moved by an even ratio of dynein and kinesin motors. This suggests that both motor systems exert similar forces. An exception is endosome motility in *D. discoideum*. Here, a single kinesin-3 counteracts many weaker dyneins in EE traffic (Soppina et al., 2009). Thus, variations exist and it is conceivable that the dynein in *U. maydis* is much stronger than kinesin-3. If this is the case, the turning from anterograde to retrograde transport upon binding of dynein could be a consequence of a tug-of-war, in which dynein overcomes the numerous kinesin-3 motors. Alternatively, dynein might deactivate kinesin-3, which could be done by interfering with its ability to interact with microtubules. This idea is supported by the observation that many organelles pause for some time after dynein unbinds. This pausing might indicate that the kinesin-3 motors are not in contact with the microtubule during dynein-based motility. Future studies need to distinguish between a difference in force generation or a deactivation of kinesin-3 by dynein binding.

5.4 Motors cooperate to allow long-range early endosomes motility

The use of photo-activatable GFP fused to the early endosome-specific small endosomal Rab5-like GTPase revealed that the endosomes travel over long distances, often connecting the growing tip and the rear septum. Considering the orientation of the microtubules in all regions of the cell, these organelles start with minus end-directed motility, but end their journey at plus ends. This suggests that both dynein and kinesin-3 are involved in this process. It was reported that dynein is the main motor for retrograde EE motility (Lenz at al., 2006), and by using a triple photoactivatable GFP fused to the dynein heavy chain it became obvious that dynein is able to run over long distances in retrograde direction. Indeed, in the absence of dynein, the early endosomes accumulate at microtubule plus ends, which is due to the unbalanced transport activity of kinesin-3. These data support the notion that dynein is the main retrograde transporter of early endosomes. However, in this thesis I show that kinesin-3 is the main motor for retrograde motility. This is possible because (1) the bi-polar array covers most of the hyphal cell and (2) because each organelle carries 3-5 kinesin-3 motors, which most likely cooperate. Indeed, it was shown that 4 kinesin motors can overcome 65 micrometers (Klumpp & Lipowsky, 2005), whereas single motors are not able to move processively over longer distances (Howard et al., 1989; Wang et al., 1995; Thorn et al., 2000; Reck-Peterson et al., 2006). Dynein, on the other hand, is not essential for long range motility, but is necessary to capture early endosomes at the plus-ends and transport them back through the distal uni-polar microtubule array near the tip and septum. Thus, both motors cooperate to ensure that EE continuously move over long distances along the non-uniform microtubule array.

5.5 Summary and outlook

Bidirectional transport of early endosomes in *U. maydis* is a stochastic process. Kinesin-3 is always on the organelle while dynein binds only transiently. At apical microtubule plus ends dynein forms comets and thereby increases the probability that an arriving EE gets loaded onto the motor. This mechanism prevents the organelle from falling off the microtubule end. The same stochastic loading process appears to happen in sub-apical regions along the microtubules. Here a single dynein wins against three to five kinesin-3 motors. This suggests that the dynein controls the activity of the kinesins when they are both on the same organelle. After the release of dynein from the early endosomes, kinesin-3 takes over and moves the organelle in either anterograde or retrograde direction. This depends on the underlying microtubule array. Thus, the stochastic binding of dynein and unbinding in combination with the organization of the microtubule array controls the bidirectional behaviour of the endosomes.

Two main questions remain unanswered. The first one is why is dynein moving over 40µm, when it is supporting EE motility for only 10-20 micrometers? One possibility is that dynein rebinds to kinesin-3-driven EE, thereby supporting retrograde motility in sub-apical regions. The residual motility in Kin3^{ts} mutant hyphae supports such a notion. This possibility could be further investigated by co-localisation of early endosomes and dynein in the central part of the hyphae. A second option is that retrograde motility of dynein in the bi-polar array reflects the activity of kinesin-1, which is thought to deliver dynein to the microtubule plus ends (Zhang et al., 2003; Lenz et al., 2006). After dynein has left the EE at 10-20 micrometre behind the tip, it could become a passive cargo on kinesin-1-

driven organelles. To follow this up, it would be necessary to visualise kinesin-1 and co-localise it with dynein on a single molecule level. In addition, a fast-reacting temperature-sensitive mutant of kinesin-1 need to be generated and the effect of kinesin-1 deactivation on retrograde dynein motility needs to be investigated.

The second main question is why the EE move over such long distances? The cellular role of the long distances EE motility is not known, but mutants defective in EE motility are defective in hyphal growth and nuclear migration (Schuchardt et al., 2005; Lenz et al., 2006). It was speculated that EE motility supports communication between the growing tip and the nucleus (Steinberg, 2007). In nerve cells, motility of EE is involved in retrograde signalling between the distal synapses and the cell body (Miaczynska et al., 2004, Howe & Mobley 2005). In this way the nucleus obtains information from the distal cell end. A similar situation might exist in hyphal cells of *U. maydis*. These cells expand at the tip and the nucleus remains positioned 40-50 µm behind the growth region (Fuchs et al., 2005), suggesting that it receives information that enables it to maintain the distance to the tip. While this is a tempting possibility, no experimental evidence for a role of EE in cell signalling in *U. maydis* exists.

References

Abenza JF, Pantazopoulou A, Rodriguez JM, Galindo A, Penalva MA (2009) Long-distance movement of *Aspergillus nidulans* early endosomes on microtubule tracks. *Traffic* 10, 57–75

Agutter PS, Wheatley DN (2000) Random walks and cell size. *Bioessays* 11, 1018-1023.

Akhmanova A, Steinmetz MO (2008) Tracking the ends: a dynamic protein network controls the fate of microtubule tips. *Nature Rev* 9, 309–322

Allan V. (1995) Protein phosphatase 1 regulates the cytoplasmic dynein-driven formation of endoplasmic reticulum networks in vitro. *J Cell Biol*. 128, 879-891.

Ally S, Larson AG, Barlan K, Rice SE, Gelfand VI (2009) Opposite-polarity motors activate one another to trigger cargo transport in live cells. *J Cell Biol* 187, 1071-1082

Alvarez-Dominguez C, Stahl PD. (1999) Increased expression of Rab5a correlates directly with accelerated maturation of *Listeria* monocytogenes phagosomes. *J Biol Chem*. 274, 11459-11462

Aniento F, Emans N, Griffiths G, Gruenberg J. (1993) Cytoplasmic dynein-dependent vesicular transport from early to late endosomes. *J Cell Biol*. 123, 1373-1387

Baas PW, Deitch JS, Black MM, Banker GA (1988) Polarity orientation of microtubules in hippocampal neurons: uniformity in the axon and nonuniformity in the dendrite. *Proc Natl Acad Sci* 85, 8335-8339

Baas PW, Slaughter T, Brown A, Black MM (1991) Microtubule dynamics in axons and dendrites. *J Neurosci Res* 30, 134-153

Banuett, F., and Herskowitz, I. (1996). Discrete developmental stages during teliospore formation in the corn smut fungus, *Ustilago maydis*. *Development* 122, 2965-2976.

Barkus RV, Klyachko O, Horiuchi D, Dickson BJ, Saxton WM (2008) Identification of an axonal kinesin-3 motor for fast anterograde vesicle transport that facilitates retrograde transport of neuropeptides. *Mol Biol Cell*. 19, 274-283.

Behnia R, Munro S. 2005 Organelle identity and the signposts for membrane traffic. *Nature* 438, 597-604.

Berón W, Alvarez-Dominguez C, Mayorga L, Stahl PD. (1995) Membrane trafficking along the phagocytic pathway. *Trends Cell Biol*. 5, 100-104.

Bloom, K. (2001). Nuclear migration: cortical anchors for cytoplasmic dynein. *Curr. Biol*. 11, 326–329.

Brady ST. (1985) A novel brain ATPase with properties expected for the fast axonal transport motor. *Nature*. 317, 73-75.

Brendza, R.P., Serbus, L.R., Duffy, J.B., and Saxton, W.M. (2000). A function for kinesin I in the posterior transport of oskar mRNA and Staufen protein. *Science* 289, 2120–2122.

Bucci, C. Parton RG, Mather IH, Stunnenberg H, Simons K, Hoflack B, Zerial M. (1992).The small GTPase rab5 functions as a regulatory factor in the early endocytic pathway. *Cell* 70, 715–728

Burton PR, Paige JL (1981) Polarity of axoplasmic microtubules in the olfactory nerve of the frog. *Proc Natl Acad Sci* 78: 3269-3273

Cai D, Hoppe AD, Swanson JA, Verhey KJ. (2007) Kinesin-1 structural organization and conformational changes revealed by FRET stoichiometry in live cells. *J Cell Biol.* 176, 51-63.

Carminati JL, Stearns T (1997) Microtubules orient the mitotic spindle in yeast through dynein-dependent interactions with the cell cortex. *J Cell Biol*, 138, 629-641.

Chada, S.R., and Hollenbeck, P.J. (2003). Mitochondrial movement and positioning in axons: the role of growth factor signaling. *J. Exp. Biol*. 206, 1985–1992.

Christoforidis S, Miaczynska M, Ashman K, Wilm M, Zhao L, Yip SC, Waterfield MD, Backer JM, Zerial M. 1999 Phosphatidylinositol-3-OH kinases are Rab5 effectors. *Nat Cell Biol* 1, 249–252.

Clarke M, Köhler J, Heuser J, Gerisch G. (2002) Endosome fusion and microtubule-based dynamics in the early endocytic pathway of *dictyostelium*. *Traffic*. 3, 791-800.

Corthesy-Theulaz I., A. Pauloin, and S.R. Pfeffer. (1992). Cytoplasmic dynein participates in the centrosomal localization of the Golgi complex. *J. Cell Biol*. 118, 1333–1345.

Culver-Hanlon TL, Lex SA, Stephens AD, Quintyne NJ, King SJ. (2006) A microtubule-binding domain in dynactin increases dynein processivity by skating along microtubules. *Nat Cell Biol*. 8, 264-270.

Deacon SW, Nascimento A, Serpinskaya AS, Gelfand VI (2005) Regulation of bidirectional melanosome transport by organelle bound MAP kinase. *Curr Biol* 15, 459–463.

Deacon SW, Serpinskaya AS, Vaughan PS, Lopez Fanarraga M, Vernos I, Vaughan KT, Gelfand VI. (2003) Dynactin is required for bidirectional organelle transport. *J Cell Biol* 160, 297–301.

DeGiorgis JA, Petukhova TA, Evans TA, Reese TS. (2008) Kinesin-3 is an organelle motor in the *squid* giant axon. *Traffic*. 9, 1867-1877.

Desai A, Mitchison TJ. (1997). Microtubule polymerization dynamics. *Annual Review of Cell and Developmental Biology* 13, 83–117.

Dixit R, Ross JL. (2010) Studying plus-end tracking at single molecule resolution using TIRF microscopy. *Methods Cell Biol*. 95, 543-554.

Feiguin, F., Ferreira, A., Kosik, K.S., and Caceres, A. (1994). Kinesinmediated organelle translocation revealed by specific cellular manipulations. *J. Cell Biol.* 127, 1021–1039.

Ferhat, L., Cook, C., Chauviere, M., Harper, M., Kress, M., Lyons, G. E., and Baas, P. W. (1998). Expression of the mitotic motor protein Eg5 in postmitotic neurons: implications for neuronal development. *J. Neurosci*. 18, 7822–7835.

Fink, G. & Steinberg, G. (2006). Dynein-dependent motility of microtubules and nucleation sites supports polarization of the tubulin array in the fungus *Ustilago maydis*. *Mol. Biol. Cell* 17, 3242–3253

Fink G, Schuchardt I, Colombelli J, Stelzer E, Steinberg G. (2006) Dynein-mediated pulling forces drive rapid mitotic spindle elongation in *Ustilago maydis*. *EMBO J.* 25, 4897-4908.

Finley KR, Bouchonville KJ, Quick A, Berman J. (2008) Dynein-dependent nuclear dynamics affect morphogenesis in *Candida albicans* by means of the Bub2p spindle checkpoint. *J Cell Sci*. 121, (Pt 5):724.

Fuchs, U., Manns, I. & Steinberg, G. (2005) Microtubules are dispensable for the initial pathogenic development but required for long-distance hyphal growth in the corn smut fungus *Ustilago maydis*. *Mol. Biol. Cell* 16, 2746–2758.

Gadde S, Heald R. (2004) Mechanisms and molecules of the mitotic spindle. *Curr Biol*. 14, R797-R805

Garcia-Muse, T., Steinberg, G., and Perez-Martin, J. (2003). Pheromone-induced G2 arrest in the phytopathogenic fungus *Ustilago maydis*. *Eukaryot. Cell* 2, 494–500.

Gibbons, I.R., and Rowe, A.J. (1965). Dynein: a protein with adenosine triphosphatase activity from cilia. *Science* 149, 424–426.

Gibson T, Musacchio A, Thompson J, Saraste M, Rice P (1993). "The PH domain: a common piece in the structural patchwork of signalling proteins". *Trends Biochem. Sci*. 18, 343–348.

Gorvel, J. P., Chavrier, P., Zerial., M. & Gruenberg, J. (1991). rab5 controls early endosome fusion in vitro. *Cell* 64, 915–925

Gross SP, Tuma MC, Deacon SW, Serpinskaya AS, Reilein AR, Gelfand VI. (2002a) Interactions and regulation of molecular motors in *Xenopus* melanophores. *J Cell Biol*. 156, 855-865.

Gross SP, Welte MA, Block SM, Wieschaus EF. (2002b) Coordination of opposite-polarity microtubule motors. *J Cell Biol*. 156, 715-724.

Gross, S. P. (2004). Hither and yon: a review of bi-directional microtubule-based transport. *Phys. Biol.* 1, 1–11

Guillaud L, Wong R, Hirokawa N (2008) Disruption of KIF17-Mint1 interaction by CaMKII-dependent phosphorylation: A molecular model of kinesin-cargo release. *Nat Cell Biol* 10, 19–29.

Hartman NC, Nye JA, Groves JT. 2009 Cluster size regulates protein sorting in the immunological synapse. *Proc Natl Acad Sci U S A*. 106, 12729-12734

Ha J, Lo KW, Myers KR, Carr TM, Humsi MK, Rasoul BA, Segal RA, Pfister KK (2008) A neuron-specific cytoplasmic dynein isoform preferentially transports TrkB signaling endosomes. *J Cell Biol* 181, 1027-1039

Habura A, Tikhonenko I, Chisholm RL, Koonce MP. (1999) Interaction mapping of a dynein heavy chain. Identification of dimerization and intermediate-chain binding domains. *J Biol Chem*. 274, 15447-1553

Hackney DD, Stock MF. (2008) Kinesin tail domains and Mg2+ directly inhibit release of ADP from head domains in the absence of microtubules. *Biochemistry*. 47, 7770-7778.

Hall, D.H., and Hedgecock, E.M. (1991). Kinesin-related gene unc-104 is required for axonal transport of synaptic vesicles in *C. elegans*. *Cell* 65, 837–847.

Hamm-Alvarez, S.F., Kim, P.Y., and Sheetz, M.P. (1993). Regulationof vesicle transport in CV-1 cells and extracts. *J. Cell Sci*. 106, 955–966

Hammond JW, Cai D, Blasius TL, Li Z, Jiang Y, Jih GT, Meyhofer E, Verhey KJ. (2009) Mammalian Kinesin-3 motors are dimeric in vivo and move by processive motility upon release of autoinhibition. *PLoS Biol.* 7, e72.

Harada A, Takei Y, Kanai Y, Tanaka Y, Nonaka S, Hirokawa N. (1998) Golgi vesiculation and lysosome dispersion in cells lacking cytoplasmic dynein. *J Cell Biol*. 141, 51-59.

Heidemann SR, Landers JM, Hamborg MA (1981) Polarity orientation of axonal microtubules. *J Cell Biol* 91, 661-665

Heil-Chapdelaine RA, Tran NK, Cooper JA. (2000) Dynein-dependent movements of the mitotic spindle in *Saccharomyces cerevisiae* Do not require filamentous actin. *Mol Biol Cell*. 11, 863-872.

Hemmings BA, Haslam RJ, Koide HB (1993). "Pleckstrin domain homology". *Nature* 363, 309–310.

Hendricks AG, Perlson E, Ross JL, Schroeder HW 3rd, Tokito M, Holzbaur EL. (2010) Motor coordination via a tug-of-war mechanism drives bidirectional vesicle transport. *Curr Biol* 20, 697–702.

Hirokawa, N. (1998). Kinesin and dynein superfamily proteins and the mechanism of organelle transport. *Science* 279, 519–526.

Hirokawa N, Takemura R (2004) Molecular motors in neuronal development, intracellular transport and diseases. *Curr Opin Neurobiol* 14, 564-573

Hirokawa, N. and Takemura, R. (2005) Molecular motors and mechanisms of directional transport in neurons. *Nat. Rev. Neurosci*. 6, 201–214

Hollenbeck, P.J. (1996). The pattern and mechanism of mitochondrial transport in axons. *Front. Biosci*. 1, d91–d102

Hollenbeck, P.J. (1993). Products of endocytosis and autophagy are retrieved from axons by regulated retrograde organelle transport. *J. Cell Biol.* 121, 305–315.

Horiguchi K, Hanada T, Fukui Y, Chishti AH. (2006) Transport of PIP3 by GAKIN, a kinesin-3 family protein, regulates neuronal cell polarity. *J Cell Biol*. 174, 425-36.

Hirokawa, N. (1998). Golgi vesiculation and lysosome dispersion in cells lacking cytoplasmic dynein. *J. Cell Biol*. 141, 51–59.

Honnappa S, Okhrimenko O, Jaussi R, Jawhari H, Jelesarov I, Winkler FK, Steinmetz MO (2006) Key interaction modes of dynamic +TIP networks. *Mol Cell* 23, 663–671

Hoogenraad, C.C., Akhmanova, A., Howell, S.A., Dortland, B.R., De Zeeuw, C.I., Willemsen, R., Visser, P., Grosveld, F., and Galjart, N. (2001). Mammalian Golgi-associated bicaudal-D2 functions in the dynein-dynactin pathway by interacting with these complexes. *EMBO J.* 20, 4041–4054

Howard J, Hudspeth AJ, Vale RD (1989) Movement of microtubules by single kinesin molecules. *Nature* 342, 154-158

Howe, C. L. (2005) Modeling the signaling endosome hypothesis: why a drive to the nucleus is better than a (random) walk. *Theor. Biol. Med. Model* 2, 43.

Januschke, J., Gervais, L., Dass, S., Kaltschmidt, J.A., Lopez-Schier, H., St Johnston, D., Brand, A.H., Roth, S., and Guichet, A. (2002). Polar transport in the Drosophila oocyte requires Dynein and Kinesin I cooperation. *Curr. Biol*. 12, 1971–1981.

Lee JR, Shin H, Choi J, Ko J, Kim S, Lee HW, Kim K, Rho SH, Lee JH, Song HE, Eom SH, Kim E. (2004) An intramolecular interaction between the FHA domain and a coiled coil negatively regulates the kinesin motor KIF1A. *EMBO J.* 23, 1506-1515.

Lee WL, Oberle JR, Cooper JA. (2003) The role of the lissencephaly protein Pac1 during nuclear migration in budding yeast. *J Cell Biol.* 160, 355-364.

Lee WL, Kaiser MA, Cooper JA. (2005) The offloading model for dynein function: differential function of motor subunits. *J Cell Biol*. 168, 201-207

Job D, Valiron O, Oakley B. (2003). Microtubule nucleation. *Current Opinions in Cell Biology* 15, 111–117.

Loubéry S, Wilhelm C, Hurbain I, Neveu S, Louvard D, Coudrier E. (2008) Different microtubule motors move early and late endocytic compartments. *Traffic*. 9, 492-509.

Kardon JR, Reck-Peterson SL, Vale RD. (2009) Regulation of the processivity and intracellular localization of Saccharomyces cerevisiae dynein by dynactin. *Proc Natl Acad Sci U S A*. 106, 5669-5674

Kämper J, Kahmann R, Bölker M, Ma LJ, Brefort T, Saville BJ, Banuett F, Kronstad JW, Gold SE, Müller O, Perlin MH, Wösten HA, de Vries R, Ruiz-Herrera J, Reynaga-Peña CG, Snetselaar K, McCann M, Pérez-Martín J, Feldbrügge M, Basse CW, Steinberg G, Ibeas JI, Holloman W, Guzman P, Farman M, Stajich JE, Sentandreu R, González-Prieto JM, Kennell JC, Molina L, Schirawski J, Mendoza-Mendoza A, Greilinger D, Münch K, Rössel N, Scherer M, Vranes M, Ladendorf O, Vincon V, Fuchs U, Sandrock B, Meng S, Ho EC, Cahill MJ, Boyce KJ, Klose J, Klosterman SJ, Deelstra HJ, Ortiz-Castellanos L, Li W, Sanchez-Alonso P, Schreier PH, Häuser-Hahn I, Vaupel M, Koopmann E, Friedrich G, Voss H, Schlüter T, Margolis J, Platt D, Swimmer C, Gnirke A, Chen F, Vysotskaia V, Mannhaupt G, Güldener U, Münsterkötter M, Haase D, Oesterheld M, Mewes HW, Mauceli EW, DeCaprio D, Wade CM, Butler J, Young S, Jaffe DB, Calvo S, Nusbaum C, Galagan J, Birren BW. (2006) Insights from the genome of the biotrophic fungal plant pathogen *Ustilago maydis*. *Nature*. 444, 97-101.

King, S.M. (2000). The dynein microtubule motor. *Biochim. Biophys. Acta* 1496, 60–75.

King, S.J., and Schroer, T.A. (2000). Dynactin increases the processivity of the cytoplasmic dynein motor. *Nat. Cell Biol*. 2, 20–24.

Klopfenstein, D.R., Tomishige, M., Stuurman, N., and Vale, R.D. (2002). Role of phosphatidylinositol(4,5)bisphosphate organization in membrane transport by the Unc104 kinesin motor. *Cell* 109, 347–358.

Klopfenstein DR, Holleran EA, Vale RD. 2003 Kinesin motors and microtubule-based organelle transport in *Dictyostelium discoideum J Muscle Res Cell Motil*. 23, 631-638

Klumpp S, Lipowsky R (2005) Cooperative cargo transport by several molecular motors. *Proc Natl Acad Sci USA* 102, 17284-17289

Kobayashi T, Murayama T. (2009) Cell cycle-dependent microtubule-based dynamic transport of cytoplasmic dynein in mammalian cells. *PLoS One*. 4, e7827

Konzack S, Rischitor PE, Enke C, Fischer R. (2004) The role of the kinesin motor KipA in microtubule organization and polarized growth of *Aspergillus nidulans*. *Mol Biol Cell*. 16, 497-506

Koval M, Pagano RE. (1989) Lipid recycling between the plasma membrane and intracellular compartments: transport and metabolism of fluorescent sphingomyelin analogues in cultured fibroblasts. *J Cell Biol*. 108, 2169-2181

Kuznetsov SA, Vaisberg YA, Rothwell SW, Murphy DB, Gelfand VI. (1989) Isolation of a 45-kDa fragment from the kinesin heavy chain with enhanced ATPase and microtubule-binding activities. *J Biol Chem.* 264, 589-595.

Larsen KS, Xu J, Cermelli S, Shu Z, Gross SP (2008) BicaudalD actively regulates microtubule motor activity in lipid droplet transport. *PLoS ONE* 3, e3763

Lee, W. L., Oberle, J. R., and Cooper, J. A. (2003). The role of the lissencephaly protein Pac1 during nuclear migration in budding yeast. *J. Cell Biol*. 160, 355–364.

Lehmler, C., Steinberg, G., Snetselaar, K.M., Schliwa, M., Kahmann, R., and Bolker, M. (1997). Identification of a motor protein required for filamentous growth in *Ustilago maydis*. *EMBO J.* 16, 3464–3473.

Lenz, J. H., Schuchardt, I., Straube, A. & Steinberg, G. (2006). A dynein loading zone for retrograde endosome motility at microtubule plus-ends. *EMBO J*. 25, 2275–2286

Ligon LA, Shelly SS, Tokito M, Holzbaur EL (2003). The microtubule plus-end proteins EB1 and dynactin have differential effects on microtubule polymerization. *Mol Biol Cell* 14, 1405–1417

Lomakin AJ, Semenova I, Zaliapin I, Kraikivski P, Nadezhdina E, Slepchenko BM, Akhmanova A, Rodionov V (2009) CLIP-170 dependent capture of membrane organelles by microtubules initiates minus-end directed transport. *Dev Cell* 17, 323–333

Maly, I.V. (2002). A stochastic model for patterning of the cytoplasm by the saltatory movement. J*. Theor. Biol*. 216, 59–71.

Manneville, J.B., Etienne-Manneville, S., Skehel, P., Carter, T., Ogden, D., and Ferenczi, M. (2003). Interaction of the actin cytoskeleton with microtubules regulates secretory organelle movement near the plasma membrane in human endothelial cells. *J. Cell Sci*. 116, 3927–3938.

McDonald, D., Vodicka, M.A., Lucero, G., Svitkina, T.M., Borisy, G.G., Emerman, M., and Hope, T.J. (2002). Visualization of the intracellular behavior of HIV in living cells. *J. Cell Biol*. 159, 441–452.

Mische S, Li M, Serr M, Hays TS. 2007 Direct observation of regulated ribonucleoprotein transport across the nurse cell/oocyte boundary *Mol Biol Cell*. 2007 18, 2254-2263

Mitchison T, Kirschner M (1984). "Dynamic instability of microtubule growth". *Nature* 312, 237–242.

Murray, J.W., Bananis, E., and Wolkoff, A.W. (2000). Reconstitution of ATP-dependent movement of endocytic vesicles along microtubules in vitro: an oscillatory bidirectional process. *Mol. Biol. Cell* 11, 419–433.

Müller MJ, Klumpp S, Lipowsky R (2008) Tug-of-war as a cooperative mechanism for bidirectional cargo transport by molecular motors. *Proc Natl Acad Sci USA* 105, 4609–4614.

Nascimento, A. A., J. T. Roland, and V. I. Gelfand. 2003. Pigment cells: a model for the study of organelle transport. *Annu. Rev. Cell Dev. Biol*. 19, 469–491

Nangaku, M., Sato-Yoshitake, R., Okada, Y., Noda, Y., Takemura, R., Yamazaki, H., and Hirokawa, N. (1994) KIF1B, a novel microtubule plus end-directed monomeric motor protein for transport of mitochondria. *Cell* 79, 1209-1220.

Nilsson, H., and M. Wallin. 1997. Evidence for several roles of dynein in pigment transport in melanophores. *Cell Motil. Cytoskeleton*. 38, :397–409

Nielsen E, Severin F, Backer JM, Hyman AA, Zerial M. (1999) Rab5 regulates motility of early endosomes on microtubules. *Nat Cell Biol*. 1, 376-382.

Nogales E, Whittaker M, Milligan RA, Downing KH (1999) High-resolution model of the microtubule. *Cell* 96, 79-88

Oakley BR. (2004) Tubulins in *Aspergillus nidulans*. *Fungal Genet Bio* l41, 420-427.

Okada, Y., Yamazaki,H., Sekine-Aizawa, Y., and Hirokawa, N. (1995). The neuron-specific kinesin superfamily protein KIF1A is a unique monomeric motor for anterograde axonal transport of synaptic vesicle precursors. *Cell* 81, 769–780.

Paschal., B.M., Shpetner, H.S., and Vallee, R.B. (1987). MAP1C is a microtubule-activated ATPase which translocates microtubules in vitro and has dynein-like properties. *J. Cell Biol*. 105, 1273–1282.

Paschal, B. M. and Vallee, R. B. (1987) Retrograde transport by the microtubule-associated protein MAP 1C. *Nature* 330, 181–183

Pedersen LB, Geimer S, Rosenbaum JL (2006) Dissecting the molecular mechanisms of intraflagellar transport in chlamydomonas. *Curr Biol* 16, 450–459.

Peñalva MÁ. 2010 Endocytosis in filamentous fungi: Cinderella gets her reward. *Curr Opin Microbiol*. 13, 684-692

Pilling AD, Horiuchi D, Lively CM, Saxton WM. 2006 Kinesin-1 and Dynein are the primary motors for fast transport of mitochondria in Drosophila motor axons. *Mol Biol Cell*. 17, 2057-68.

Prahlad, V., Yoon, M., Moir, R.D., Vale, R.D., and Goldman, R.D. (1998). Rapidmovements of vimentin onmicrotubule tracks: kinesin- dependent assembly of intermediate filament networks. *J. Cell Biol*. 143, 159–170.

Rebhun, L.I. (1972). Polarized intracellular particle transport: salutatory movements and cytoplasmic streaming. *Int. Rev. Cytol*. 32, 93–137.

Reck-Peterson SL, Yildiz A, Carter AP, Gennerich A, Zhang N, Vale RD (2006) Single-molecule analysis of dynein processivity and stepping behavior. *Cell* 126, 335-348

Roca MG, Kuo HC, Lichius A, Freitag M, Read ND. (2010) Nuclear dynamics, mitosis, and the cytoskeleton during the early stages of colony initiation in *Neurospora crassa*. *Eukaryot Cell.* 8, 1171-1183

Rogers, S. L., and V. I. Gelfand. 1998. Myosin cooperates with microtubule motors during organelle transport in melanophores. *Curr. Biol*. 8, 161–164.

Samso, M., Radermacher, M., Frank, J., and Koonce, M.P. (1998). Structural characterization of a dynein motor domain. *J. Mol. Biol.* 276, 927–937.

Scholey JM, Porter ME, Grissom PM, McIntosh JR. (1985) Identification of kinesin in sea urchin eggs, and evidence for its localization in the mitotic spindle. *Nature.* 318, 483-486.

Scholey JM (2003) Intraflagellar transport. *Annu Rev Cell Dev Biol* 19, 423–443.

Schuchardt I, Assmann D, Thines E, Schuberth C, Steinberg G (2005) Myosin-V, Kinesin-1, and Kinesin-3 cooperate in hyphal growth of the fungus *Ustilago maydis*. *Mol Biol Cell*. 16, 5191-5201

Schroer TA, Sheetz MP. (1991) Two activators of microtubule-based vesicle transport. *J Cell Biol*. 5, 1309-1318.

Seabra MC, Coudrier E. (2004) Rab GTPases and myosin motors in organelle motility *Traffic.* 5, 393-399.

Seiler S, Nargang FE, Steinberg G, Schliwa M. (1997) Kinesin is essential for cell morphogenesis and polarized secretion in *Neurospora crassa*. *EMBO J*. 16, 3025-3034.

Seiler S, Kirchner J, Horn C, Kallipolitou A, Woehlke G, Schliwa M. (2000) Cargo binding and regulatory sites in the tail of fungal conventional kinesin. *Nat Cell Biol*. 6, 333-338.

Sheeman B, Carvalho P, Sagot I, Geiser J, Kho D, Hoyt MA, Pellman D. (2003) Determinants of *S. cerevisiae* dynein localization and activation: implications for the mechanism of spindle positioning. *Curr Biol*. 13, 364-372.

Shimmen T. (2007) The sliding theory of cytoplasmic streaming: fifty years of progress. *J Plant Res*. 120, 31-43.

Shubeita GT, Tran SL, Xu J, Vershinin M, Cermelli S, Cotton SL, Welte MA, Gross SP. (2008) Consequences of motor copy number on the intracellular transport of kinesin-1-driven lipid droplets. *Cell* 135, 1098–1107.

Smith, G.A., Gross, S.P., and Enquist, L.W. (2001). Herpesviruses use bidirectional fast-axonal transport to spread in sensory neurons. *Proc. Natl. Acad. Sci. USA* 98, 3466–3470.

Soldati T, Schliwa M. 2006. Powering membrane traffic in endocytosis and recycling. *National Review of Molecular Cell Biology* 7, 897–908.

Soppina V, Rai AK, Ramaiya AJ, Barak P, Mallik R (2009) Tug-of-war between dissimilar teams of microtubule motors regulates transport and fission of endosomes. *Proc Natl Acad Sci USA* 106, 19381-19386

Steinberg G, Schliwa M. (1995) The *Neurospora* organelle motor: a distant relative of conventional kinesin with unconventional properties. *Mol Biol Cell*. 6, 1605-1618

Steinberg G, Schliwa M. (1996) Characterization of the biophysical and motility properties of kinesin from the fungus *Neurospora crassa*. *J Biol Chem*. 271, 7516-7521.

Steinberg G. (1997) A kinesin-like mechanoenzyme from the zygomycete Syncephalastrum racemosum shares biochemical similarities with conventional kinesin from *Neurospora crassa*. *Eur J Cell Biol*. 73, 124-131.

Steinberg G, Schliwa M, Lehmler C, Bölker M, Kahmann R, McIntosh JR. (1998) Kinesin from the plant pathogenic fungus *Ustilago maydis* is involved in vacuole formation and cytoplasmic migration. *J Cell Sci*. 111, 2235-2246.

Steinberg G, Wedlich-Söldner R, Brill M, Schulz I (2001) Microtubules in the fungal pathogen *Ustilago maydis* are highly dynamic and determine cell polarity. *J Cell Sci* 114, 609–622

Steinberg G. (2007) On the move: endosomes in fungal growth and pathogenicity. *Nat Rev Microbiol*. 5, 309-316.

Steinberg G, Perez-Martin J.(2008) *Ustilago maydis*, a new fungal model system for cell biology. *Trends Cell Biol*. 18, 61-67. Review.

Straube A, Enard W, Berner A, Wedlich-Söldner R, Kahmann R, Steinberg G. (2001) A split motor domain in a cytoplasmic dynein. *EMBO J*. 20, 5091-5100.

Straube, A., Brill, M., Oakley, B. R., Horio, T. & Steinberg, G. (2003). Microtubule organization requires cell cycle-dependent nucleation at dispersed cytoplasmic sites: polar and perinuclear microtubule organizing centers in the plant *pathogen Ustilago maydis*. *Mol. Biol. Cell* 14, 642–657

Sun S, Siglin A, Williams JC, Polenova T. (2009) Solid-state and solution NMR studies of the CAP-Gly domain of mammalian dynactin and its interaction with microtubules. *J Am Chem Soc*. 131, 10113-10126.

Thorn KS, Ubersax JA, Vale RD (2000) Engineering the processive run length of the kinesin motor. *J Cell Biol* 151, 1093-1100

Tomishige, M., Klopfenstein, D.R., and Vale, R.D. (2002). Conversion of Unc104/KIF1A kinesin into a processive motor after dimerization. *Science* 297, 2263–2267.

Tsujikawa M, Omori Y, Biyanwila J, Malicki J. (2007) Mechanism of positioning the cell nucleus in vertebrate photoreceptors. *Proc Natl Acad Sci U S A*. 104, 14819-14824

Tuma, M. C., A. Zill, N. Le Bot, I. Vernos, and V. Gelfand. 1998. Heterotrimeric kinesin II is the microtubule motor protein responsible for pigment dispersion in *Xenopus melanophores*. *J. Cell Biol*. 143, 1547–1558.

Tynan SH, Gee MA, Vallee RB. (2000) Distinct but overlapping sites within the cytoplasmic dynein heavy chain for dimerization and for intermediate chain and light intermediate chain binding. *J Biol Chem*. 275, 32769-32774.

Tynan, S.H., Purohit, A., Doxsey, S.J., and Vallee, R.B. (2000). Light intermediate chain 1 defines a functional subfraction of cytoplasmic dynein which binds to pericentrin. *J. Biol. Chem*. 275, 32763–32768.

Vale, R.D., Reese, T.S., and Sheetz, M.P. (1985). Identification of a novel force-generating protein, kinesin, involved in microtubuleity based motility. *Cell 42*, 39–50.

Vale RD (2003) The molecular motor toolbox for intracellular transport. *Cell* 112, 467-480

Valetti C, Wetzel DM, Schrader M, Hasbani MJ, Gill SR, Kreis TE, Schroer TA (1999) Role of dynactin in endocytic traffic: effects of dynamitin overexpression and colocalization with CLIP-170. *Mol Biol Cell* 10, 4107–4120

Vaughan PS, Miura P, Henderson M, Byrne B, Vaughan KT (2002) A role for regulated binding of p150(Glued) to microtubule plus ends in organelle transport. *J Cell Biol* 158, 305–319

Vaughan KT (2005) Microtubule plus ends, motors, and traffic of Golgi membranes. *Biochim Biophys Acta* 1744, 316–324

Wacker, I., Kaether, C., Kromer, A., Migala, A., Almers, W., and Gerdes, H.H. (1997). Microtubule-dependent transport of secretory vesicles visualized in real time with a GFP-tagged secretory protein. *J. Cell Sci*. 110, 1453–1463.

Vits H. (1991) Some geometrical considerations on membrane insertion by exocytosis. *Biosystems*. 25,251-257.

Wang Z, Khan S, Sheetz MP (1995) Single cytoplasmic dynein molecule movements: characterization and comparison with kinesin. *Biophys J* 69, 2011-2023

Wang DS, Shaw G. (1995). "The association of the C-terminal region of beta I sigma II spectrin to brain membranes is mediated by a PH domain, does not require membrane proteins, and coincides with a inositol-1,4,5 triphosphate binding site." *Biochem Biophys Res Commun* 217, 608–615.

Wedlich-Söldner, R., Bölker, M., Kahmann, R. & Steinberg, G. (2000) A putative endosomal t-SNARE links exo- and endocytosis in the phytopathogenic fungus *Ustilago maydis*. *EMBO J*. 19, 1974–1986

Wedlich-Söldner R, Straube A, Friedrich MW, Steinberg G. (2002a) A balance of KIF1A-like kinesin anddynein organizes early endosomes in the fungus *Ustilago maydis*. *EMBO J*. 21, 2946–2957

Wedlich-Söldner R, Schulz I, Straube A, Steinberg G. (2002b) Dynein supports motility of endoplasmic reticulum in the fungus *Ustilago maydis*. *Mol Biol Cell*. 3, 965-977.

Weisbrich A, Honnappa S, Jaussi R, Okhrimenko O, Frey D, Jelesarov I, Akhmanova A, Steinmetz MO. (2007) Structure-function relationship of CAP-Gly domains. *Nat Struct Mol Biol*. 10, 959-967.

Welte MA, Gross SP, Postner M, Block SM, Wieschaus EF (1998) Developmental regulation of vesicle transport in Drosophila embryos: Forces and kinetics. *Cell* 92, 547–557.

Welte, M. A. (2004). Bidirectional transport along microtubules. *Curr. Biol*. 14, 525–537

Welte MA, et al. (2005) Regulation of lipid-droplet transport by the perilipin homolog LSD2. *Curr Biol* 15, 1266–1275.

Welte MA, Gross SP. (2008) Molecular motors: a traffic cop within? *HFSP J.* 2, 178-182.

Wu Q, Sandrock TM, Turgeon BG, Yoder OC, Wirsel SG, Aist JR. (1998) A fungal kinesin required for organelle motility, hyphal growth, and morphogenesis. *Mol Biol Cell.* 9, 89-101.

Xiang X, Han G, Winkelmann DA, Zuo W, Morris NR. (2000) Dynamics of cytoplasmic dynein in living cells and the effect of a mutation in the dynactin complex actin-related protein Arp1. *Curr Biol.* 10, 603-606.

Xiang X (2003) LIS1 at the microtubule plus end and its role in dynein-mediated nuclear migration. *J Cell Biol* 160, 289–290

Xiang X, Plamann M. 2003. Cytoskeleton and motor proteins in filamentous fungi. *Current Opinions in Microbiology* 6, 628–633.

Yeh E, Skibbens RV, Cheng JW, Salmon ED, Bloom K (1995) Spindle dynamics and cell cycle regulation of dynein in the budding yeast, *Saccharomyces cerevisiae*. *J Cell Biol*, 130, 687-700.

Yonekawa, Y., Harada, A., Okada, Y., Funakoshi, T., Kanai, Y., Takei, Y., Terada, S., Noda, T., and Hirokawa, N. (1998). Defect in synaptic vesicle precursor transport and neuronal cell death in KIF1A motor protein-deficient mice. *J. Cell Biol*. 141, 431–441.

Yu, W., Cook, C., Sauter, C., Kuriyama, R., Kaplan, P. L., and Baas, P. W. (2000). Depletion of a microtubule-associated motor protein induces the loss of dendritic identity. *J. Neurosci*. 20, 5782–5791.

Zhang J, Li S, Fischer R, Xiang X (2003) Accumulation of cytoplasmic dynein and dynactin at microtubule plus ends in *Aspergillus nidulans* is kinesin dependent. *Mol Biol Cel*l 14, 1479–1488

Zhang J, Zhuang L, Lee Y, Abenza JF, Pen˜alva MA, Xiang X (2010) The microtubule plus-end localization of Aspergillus dynein is important for dynein-early-endosome interaction but not for dynein ATPase activation. *J Cell Sci* 123, 3596–3604

Zhang Y. (2009) Properties of tug-of-war model for cargo transport by molecular motors. *Phys Rev E Stat Nonlin Soft Matter Phys.* 79, 061918.

Zheng Y, Wildonger J, Ye B, Zhang Y, Kita A, Younger SH, Zimmerman S, Jan LY, Jan YN (2008) Dynein is required for polarized dendritic transport and uniform microtubule orientation in axons. *Nature cell biology* 10, 1172-1180